Aspects of Work in Quantum Thermodynamics



Cormac Browne

St. Edmund's Hall

University of Oxford

A thesis submitted for the degree of

Doctor of Philosophy

Trinity 2017

For My Family

Abstract

Landauer's principle states that it costs at least $k_{\mathrm{B}}T\ln 2$ of work to reset one bit in the presence of a heat bath at temperature T. The bound of $k_{\mathrm{B}}T\ln 2$ is achieved in the unphysical infinite-time limit. Here we consider two different finite-time protocols - one with discretised time and the second in the continuous limit. We prove analytically that the discrete time protocol enables one to reset a bit with a work cost close to $k_{\mathrm{B}}T\ln 2$ in a finite time. We construct an explicit protocol that achieves this, which involves thermalising and changing the system's Hamiltonian so as to avoid quantum coherences. Using concepts and techniques pertaining to single-shot statistical mechanics, we furthermore prove that the heat dissipated is exponentially close to the minimal amount possible not just on average, but guaranteed with high confidence in every run. Moreover we exploit the protocol to design a quantum heat engine that works near the Carnot efficiency in finite time. We further contrast this to a continuous time version of the protocol which is substantially less energy sufficient. We also consider the fluctuations in the work cost, and calculate how their magnitude is suppressed by a factor depending on the length of the protocol.

We demonstrate with an experiment how molecules are a natural test-bed for probing fundamental quantum thermodynamics. Single-molecule spectroscopy has undergone transformative change in the past decade with the advent of techniques permitting individual molecules to be distinguished and probed. By considering the time-resolved emission spectrum of organic molecules as arising from quantum jumps between states, we demonstrate that the quantum Jarzynski equality is satisfied in this set-up. This relates the heat dissipated into the environment to the free energy difference between the initial and final state. We demonstrate also how utilizing the quantum Jarzynski equality allows for the detection of energy shifts within a molecule, beyond the relative shift.

Acknowledgements

Firstly, I wish to thank Oscar Dahlsten for his enormous contribution to my studies whilst at Oxford University. Without his guidance and assistance the completion of this work would not have been possible. I would like to thank my supervisor, Vlatko Vedral, for all of the discussions and idea-generation session which enabled so much of my progress. Furthermore I am grateful to Andrew Garner, Felix Binder, Felix Pollock, Benjamin Yadin, Thomas Elliot and Anu Unnikrishnan for all of the time spent chatting about physics and everything else in the office.

I am also incredibly glad of all of the support I have received from my family and non-academic friends throughout this endeavour. Especial thanks belong to my parents, for always encouraging inquisitiveness, learning and teaching me that no goal is unachievable.

Finally, I would like to acknowledge funding from the EPSRC which made this project feasible, as well as both the TherMiq and COST MP1209 networks which introduced me to many fantastic physicists.

Notations

k_{B}	Boltzmann's constant.
β	Defined as $(k_{\mathrm{B}}T)^{-1}$, known as the inverse temperature.
$\langle\cdot\rangle$	The expecation value of a quantity.
$\mathbb{1}$	The identity matrix.
$\mathbf{a}$	Vectors are denoted by bold font.
$\rightarrow$	Indicates a transition or mapping from one object to another.
$\neg$	Denotes the not operation.
E	Internal energy of a system (normally denoted by U).
E_i	The energy of a particular part of a system.
W	Work.
Q	Heat.
$đx$	Inexact differential of some quantity, x.
H	Entropy, typically presented with an indicator of which entropy is considered.
U	A unitary evolution matrix.

Contents

Notations **iv**

List of Figures **vii**

1 Introduction **1**
- 1.1 Equilibrium Thermodynamics . . . 2
- 1.2 Out-of-Equilibrium Thermodynamics . . . 4
  - 1.2.1 Fluctuation Relations . . . 4
  - 1.2.2 Single-shot Thermodynamics . . . 6
- 1.3 Connecting Information Theory and Thermodynamics . . . 8
- 1.4 Contribution . . . 10

2 Extending Landauer's Principle to Finite Time Domains **12**
- 2.1 Introduction . . . 12
- 2.2 Performing a Quasistatic Bit Reset . . . 13
- 2.3 Extending the Protocol to Finite Time . . . 15
  - 2.3.1 The Effects of Quantum Coherence . . . 15
  - 2.3.2 Partial Thermalisation as a Partial Swap . . . 17
- 2.4 The Average Work Cost . . . 19
  - 2.4.1 Bounding the Trace-Distance . . . 19
  - 2.4.2 Bounding the Average Work Cost . . . 20
  - 2.4.3 Single-Shot Work Cost . . . 21
  - 2.4.4 Calculating $W_{\max}^{\epsilon}$. . . . 22
  - 2.4.5 Reset Error is Exponentially Suppressed . . . 23
- 2.5 A Two Level Engine in Finite Time . . . 24
  - 2.5.1 Work Extractable in Finite Time . . . 25
  - 2.5.2 Speed Limit for Positive Power Output . . . 26

2.5.3 Near-Carnot Efficiency in Finite Time 27
2.6 A Continuous Time Protocol 28
2.6.1 Bounding the Single-Shot Work Cost 31
2.7 Conclusion 32

3 Organic Molecules as an Experimental Testbed for Quantum Thermodynamics 34
3.1 Introduction 34
3.2 Fluctuation Relations for Two-Level Molecule 36
3.2.1 Jarzynski Work Relation 39
3.2.2 Crooks' Relation 40
3.2.3 Using Jarzynski to Measure Energy Shifts 41
3.3 Quantum Jump Model of a Laser-Pumped Two-Level Molecule 42
3.3.1 With a Mixed Initial State 42
3.3.2 With a Coherent Initial State 46
3.4 A Description of the Experiment 50
3.5 Mapping Experiment to Theory 53
3.6 Conclusion 56

4 Conclusions 59

A Further Details 62
A.1 Avoiding Quantum Coherences 62
A.2 Active Reversal of the Cost of Coherent Excitations 65
A.3 Bounding the Average Work Cost 67
A.4 Single-Shot Work Cost 69
A.5 Calculating $W^{\epsilon}_{\max}$. 75
A.6 A Continuous Time Protocol 76
A.7 Bounding the Average Work for a Continuous Protocol 78

Bibliography 81

List of Figures

1.1 **Schematic of single-shot work.** This figure graphically depicts one of the basic quantities of interest in single-shot thermodynamics - what is the value of work which only has probability ϵ to be exceeded. 6

2.1 **'Bit reset' by raising $\mathbf{E_2}$ to infinity.** The numbers indicate the occupation probability for the energy levels. We consider the extension of this protocol, running in finite time. 14

2.2 **A few steps of the discrete time protocol.** Thermal (dashed) and actual (solid) upper energy level populations with respect to time. At each time, $t(n)$, the upper energy level is raised, altering the thermal state. 17

2.3 **An example probabilistic work distribution.** Work values are always below $W_{\max}^{\epsilon}$, except with probability of failure ϵ given by the area of the shaded region on the right. The sum of the areas of both the shaded regions on the left and right indicates the probability of failing to be within ω of $\langle W \rangle$ (as given by Eq. 2.15). 21

2.4 **Entropy-temperature diagram for the engine cycle.** The block shaded area shows the net work exchanged by the system, which is less than that of the quasistatic (Carnot) cycle shown by the dashed rectangle filled with dots behind. For illustrative purposes, the number of energy level adjustments has been greatly reduced, and size of the associated shifts in temperature greatly exaggerated. 26

3.1 **A sample of the different trajectories** the system can take after interacting with the environment several times, aftering having been initialized in a mixed state. 45

3.2 **A sample of the different trajectories** the system can take after interacting with the environment several times, after having been initialized with a coherent state. The normalization factors, N_{i}, are simply given by the square root of the probability of each branch. 49

3.3 **Schematic of a two-level molecule** driven by laser pulses generating single photons from decaying electronic states with our thermodynamical representation of the process below it. 51

3.4 **(a)** Dibenzoterrylene (DBT) and anthracene structures consist of corrugated planar assemblies of aromatic hydrocarbons. **(b)** The energy level structure of DBT **(c)** Waveform of the decay of excited electronic states in DBT at a temperature of 4K obtained by time-resolved fluorescence spectroscopy. The waveform represents a probability distribution of the arrival times of single photons from the decaying state rather than the shape of an optical signal. 54

3.5 **Heat distribution and the Jarzynski equality** for an organic molecule undergoing spontaneous emission at a range of different temperatures. The solid curve is the result of overlaying the theoretical prediction of $\langle e^{-\beta(\Delta U - Q)} \rangle = 1$ with the experimentally calculated value. The two results have such close agreement it is not possible to distinguish between them, demonstrating that the Jarzynski equality holds for all times during the emission. The lower dashed curve represents part of the heat distribution, which has been calculated directly from the spectroscopic data. The other component of the heat distribution is simply the reverse of the presented quantity, as can be seen from $P(Q = -\Delta E) = 1 - P(Q = \Delta E)$. This is generated from the spectroscopic data by considering the cumulative number of photons emitted up to a particular time and renormalizing by the total number of photons. 55

3.6 **Value of the swapping parameter $\langle |\mu|^2 \rangle$ against time and temperature.** This parameter controls how much of a partial swap is performed after each interaction with the environment. As can be seen this is very stable for the majority of the time during the experiment, indicating that the model we employ to interpret the data is sound, see Eq. 3.34. The variation towards the end of time period for the experiment is an artifact from the experiment occupying finite time so does not perfectly map to an exponential decay. 57

A.1 **Coherent excitation.** (a) shows the state in the Bloch sphere of the initial Hamiltonian, and (b) of the final. The state ρ, diagonal in the initial Hamiltonian, is a *coherently excited* state in the final Hamiltonian. The same passive transformation U between initial and final Hamiltonians can be applied actively on ρ to map it to ρ', compensating for the work cost of coherent excitation. 65

A.2 **An example probabilistic work distribution.** A repeat of 2.3 for clarity. Work values are always below $W_{\max}^{\epsilon}$, except with probability of failure ϵ given by the area of the shaded region on the right. The sum of the areas of both the shaded regions on the left and right indicates the probability of failing to be within ω of $\langle W \rangle$ (as given by Eq. 2.15). 70

The law that entropy always increases holds, I think, the supreme position among the laws of Nature. If someone points out to you that your pet theory of the universe is in disagreement with Maxwell's equations — then so much the worse for Maxwell's equations. If it is found to be contradicted by observation — well, these experimentalists do bungle things sometimes. But if your theory is found to be against the second law of thermodynamics I can give you no hope; there is nothing for it but to collapse in deepest humiliation.

Sir Arthur Stanley Eddington[1]

Information is Physical.

Rolf Landauer[2]

1 Introduction

We begin this thesis with a short discussion on the theory of thermodynamics and those extensions to the theory which this thesis builds upon. Namely, we consider the basic fluctuation relations, the modifications to single-shot thermodynamics and the connection between thermodynamics and information. With this background presented, we move on to answer two different questions of interest. Firstly, if we are only allowed to erase information in a finite amount of time then how much energy do we need to invest to carry out this task? Furthermore, what are the variations in this value, and what determines their magnitude? Secondly, how can one test the large amount of theoretical results that have been found in quantum thermodynamics? Is it possible to adapt existing experiments to this end? We end the chapter with a brief summary of the contributions we have made towards answering these questions.

Our goal in this chapter is not to over-lengthen this thesis by retreading ground which has been well covered by many excellent textbooks and reviews. Instead we aim to provide the necessary context for the subsequent chapters, and to briefly touch upon any concepts which will show up again later. We hope the reader will trust us when we claim that this thesis should be accessible to any physicist in their first year of postgraduate studies, and that any approaches which require further explanation will receive it when they are employed. Finally we would like to note that despite the use of 'we' throughout this thesis the work contained within is the author's sole work unless otherwise indicated.

1.1 Equilibrium Thermodynamics

Originally a phenomenological theory born from the industrial revolution, the field of thermodynamics has grown to be both an immensely important practical theory, as well as one of great fundamental relevance. In the 18th and 19th centuries it found great success in explaining the operation of mechanical devices such as steam engines. It has since grown to offer insight into the entire spectrum of modern physics - from stellar objects like black holes and stars to the fully quantum regime of trapped ions or ultra-cold atoms. As stated, we do not wish this introduction to be a lengthy reiteration of previously stated information - to that end we direct the reader to the substantial range of modern textbooks dealing with equilibrium thermodynamics from a range of perspectives such as [3, 4, 5, 6, 7, 8] and here state the basic premises and key equations we will make use of later.

No discussion on equilibrium thermodynamics would be complete without first addressing what have come to be known as the laws of thermodynamics:

0. States can exist in thermal equilibrium. If state A is in equilibrium with states B

and C independently then states B and C are also in equilibrium with each other.

1. Changes in the internal energy, E, of a closed system always equal the amount of energy added or removed from the system. Furthermore, these changes can be divided into two types of energy - work, W, and heat, Q:

$$\delta E = đW + đQ \tag{1.1}$$

2. No process is possible whose sole result is the complete conversion of heat into work.

3. A system which is at temperature of absolute zero has an entropy of zero. It is impossible to cool a system to absolute zero in a finite number of steps and finite amount of time using thermodynamic methods.

From these fundamental building blocks the rest of equilibrium thermodynamics can be derived, as can be seen in the texts referenced above. As discussed, the study of engines played a large role in the early years of thermodynamics. Later in this thesis we will make use of a key result from these investigations - the Carnot efficiency. Put simply, the Carnot efficiency, η_C, represents the maximum efficiency that can be obtained by any heat engine which operates between two temperatures, T_C and T_H, and is given by $\eta_C = 1 - \frac{T_C}{T_H}$.

An alternative approach to the foundations of equilibrium thermodynamics can be found by considering the theory of statistical mechanics. Statistical mechanics derives the results of thermodynamics by first considering the microscopic states of the system and applying statistical methods to determine macroscopic properties. Throughout this thesis we will draw on this concept of considering the microscopic states to determine thermodynamic quantities.

1.2 Out-of-Equilibrium Thermodynamics

Having established the basics of equilibrium thermodynamics, we now present some of the key results in out of equilibrium thermodynamics. This is a rich area of ongoing research that seeks to apply both classical and quantum thermodynamics to more realistic situations where the processes are no longer restricted to being quasistatic, or completely described by equations of state. In this thesis we concern ourselves with fluctuation relations and single-shot thermodynamics.

Fluctuation relations are a method of connecting equilibrium variables of state with out of equilibrium quantities. Perhaps the most well known of these are the Jarzynski equality, [9], and Crooks' Fluctuation relation [10, 11], however there are many more as discussed in [12, 13].

Single-shot thermodynamics has two distinct sub-groupings - one of these is principally concerned with the tails of distributions rather than their moments, examples of this approach are [14, 15, 16]. The second approach is to consider a resource-theoretic framework, where more complex operations are derived from a set of 'free' operations and states which are given to you, see [17, 18, 19, 20].

1.2.1 Fluctuation Relations

Fluctuation relations constitute a large class of equations which aim to connect some observable quantity concerning the state of an out of equilibrium system with an equilibrium variable of state. The first of these we will discuss is the Jarzynski equality, which concerns a working medium which is driven by some external control parameter. Clearly, if this external control parameter is varied quasistatically and we perform an ensemble average, then the work will exactly equal the free energy change, ΔF. If instead this driving is done in some finite time then on average the work will depend

on the exact path (or trajectory) taken, and will in general exceed ΔF. This is just a different statement of the second law, $\langle W \rangle \geq \Delta F$.

The Jarzynski equality instead takes this inequality and replaces it with an equality that holds regardless of the protocol speed:

$$\langle \mathrm{e}^{-\beta W} \rangle = \mathrm{e}^{-\beta \Delta F} \tag{1.2}$$

Here β is the usual inverse temperature of the surrounding heat bath and W is the amount of work performed along the individual trajectories. Once again, the average taken here is an ensemble average over many runs of the protocol. This enables a suitably designed experiment to determine equilibrium properties of a system using out-of-equilibrium measurements [21, 22, 23, 24].

In discussing the Jarzynski relation we briefly mentioned different trajectories the system could take. This brings us to the second fluctuation relation of interest - Crooks' relation. Consider a thermal state which undergoes some 'forward' time-evolution under a Hamiltonian which produces some internal energy change, ΔE, which constitutes the work performed along this path, W. Now, we repeat this process multiple times so that we can define a 'forward' probability distribution of work, $p_F(W)$. It is possible to construct the time-reversed process which produces a work cost of $-W$ and a corresponding 'reverse' probability distribution, $p_R(-W)$. We can now state Crooks' relation [10, 11]:

$$\frac{p_F(W)}{p_R(-W)} = \mathrm{e}^{\beta(W-\Delta F)}. \tag{1.3}$$

We have barely scratched the surface of the large body of fluctuation relations that exist. For further reading we direct you to [25], which presents a good overview of the recent research, and some of the more recent results [26, 27, 28]. Finally, we

note that by applying Jensen's inequality ($\phi(\langle X\rangle) \leq \langle\phi(X)\rangle$, where $\phi(x)$ can be any convex function, see [29]) to Jarzynski's equality we find $\langle W\rangle \geq \Delta F$ and so it can be seen as a generalization of the second law.

1.2.2 Single-shot Thermodynamics

One branch of single-shot thermodynamics considers what thermodynamic relations and operations can be derived if you start from a framework which considers:

1. Bringing in an ancillary state drawn from the thermal distribution,
2. Conducting global, energy-conserving unitary operations encompassing the system and ancilla,
3. Discarding the evolved ancilla state,

as free operations which can be performed at no cost. This basic framework can be expanded upon in many ways to probe different questions of interest.

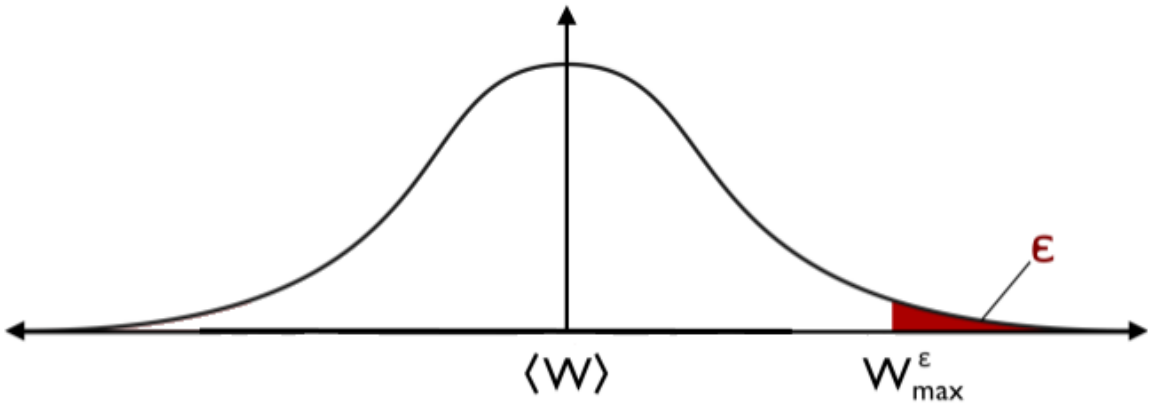


Figure 1.1: Schematic of single-shot work. *This figure graphically depicts one of the basic quantities of interest in single-shot thermodynamics - what is the value of work which only has probability ϵ to be exceeded.*

In this thesis we are concerned with the other branch, in which the focus is on what happens on a particular run of a protocol or experiment rather than considering what the average behaviour is. This is motivated by focusing on risk or fault tolerance scenarios, where we are concerned with the probability that some result is less or greater than a specified amount. This is natural to consider when we are concerned with situations where there is a minimum activation cost or where exceeding a certain work input would permanently alter/damage the working medium. An introduction to this approach can be found in [30], although the main principles are summarised here.

To understand the central question of the single-shot approach, consider taking a result at random from some probability distribution of outcomes. We then ask, up to some small probability ϵ what is the minimum/maximum value this result can be. For the case of work investiture this is depicted graphically in Fig. 1.1, and shows that the single shot quantity W^{ϵ} is defined such that the probability of requiring work W greater than this is ϵ. To provide answers to this question, single-shot thermodynamics combines techniques developed in single-shot information theory [31] with the work-extraction framework discussed in [32]. Some interesting results employing this method can be found in [14, 15, 16]. This thesis is similar in spirit to these previous works, in that we employ the work-extraction framework to understand how the probability distributions behave. However, instead of making use of the information-theoretic entropies as has been done previously we engage with the probabilities directly, and provide bounds on their possible values.

1.3 Connecting Information Theory and Thermodynamics

The connection between information and energy is perhaps obvious - it can easily be seen by considering the action of a windmill, for example. If you know which direction the wind blows (a piece of information) then it possible to extract work (energy) from it by appropriate construction of a windmill. However, despite this qualitative understanding of the connection substantial work has been done in transforming this to a more quantitative framework. The first of these is found in Maxwell's Theory of Heat, [33], wherein he postulates that a being capable of distinguishing individual gas particles and their momenta could act to violate the second law. This dæmon resides in a box, partitioned in half with a trapdoor connecting each volume and observes a gas initially at uniform temperature. By observing the gas, and opening the trapdoor when a 'hot' particle is incoming from one side or a 'cold' particle arrives from the other the dæmon can create a temperature imbalance where previously there was none.

If this were possible it would contravene the second law of thermodynamics and so led to a large body of discussion and research attempting to 'exorcise' Maxwell's dæmon. In order to tackle this problem more concretely, in 1929 Leo Szilard proposed a simple, one-molecule engine operated by an intelligent being [34]. This engine allowed Szilard to identify that measurement was required to correctly operate the engine and he associated some component of measurement (the act, remembering the data, or the forgetting) with the production of an irreversible amount of energy to balance the work gained. Following Szilard's paper there was much discussion both for and against his interpretation - many viewed the attempt to link subjective knowledge to an objective entropy as invalid. A thorough compilation of the support and criticisms written, and indeed the entire topic of Maxwell's dæmon and its subsequent evolution

can be found in Maxwell's Demon by Leff and Rex, [35].

Subsequently to this, Brillouin [36, 37] attempted to demonstrate that it was the act of measurement that produced the associated entropy increase. He did this by assuming that it was light that was needed to enable the measurement, and to distinguish this from the existing background radiation imposed limits on the amount of energy required to perform the measurement. This lead to a temporary exorcism of Maxwell's dæmon as it was held that the act of acquiring any information with which to perform the filtering of particles produced an associated entropy cost. However, once again there was criticism of the approach, and of the 'unphysical' nature of the entropies used in the analysis.

An alternative approach was presented by Landauer in 1961, [38], which instead focused on the discarding of information. He examined the situation where all effects of the measurement except its memory could be neglected and by considered the relation between logical and thermodynamical irreversibility. He argued that any process which is not logically irreversible could also be made thermodynamically reversible and thus had no intrinsic entropic cost. The only process which could not be made logically reversible was the erasure of the memory of the operating device. It is this erasure which that leads to the production of $k_{\mathrm{B}}T\ln 2$ work in the quasistatic operation of Szilard's engine and similar devices.

Following Landauer's original work, much has been done in investigating the role of memory and information in thermodynamics and the energetics of computation. These include studies on autonomous Maxwell's dæmons (e.g. [39, 40, 41, 42]), operating Maxwell's dæmons with mutual information (e.g. [43, 44, 45, 46]) and probing quantum effects on its operation (e.g. [47, 48, 49, 50, 51]). Recently there have been some experiments which approach Landauer's bound [52, 53, 54, 55]. It is within this context, and hopefully contributing to this body of research, we present Chapter 2.

1.4 Contribution

We are now in a position to briefly summarise the contributions contained within this thesis. Here we would like to spend a few sentences on discussing what we believe quantum thermodynamics to be. In our opinion, there are two closely related, but distinct investigations which occur under the banner of quantum thermodynamics. Firstly, we have the establishment of a thermodynamic theory from quantum mechanical underpinnings - that is, replacing the standard classical axioms with quantum mechanical ones and attempting to build thermodynamics out if these pieces. Secondly, we can go in the opposite direction - to what extent can we apply classical thermodynamics applies to quantum mechanical objects. That is how far down does thermodynamics, as we already understand it, go? In this thesis we are primarily concerned with the latter type of investigations - much of the thermodynamics is identical to out-of-equilibrium classical thermodynamics but is instead applied to systems which obey quantum mechanical relations.

In Chapter 2 we discuss extending Landauer's principle to finite time domains. We analyse two protocols - one consisting of discrete steps and the other a continuous process. For the discrete protocol we show that it is possible to perform the reset at an energy cost close to Landaeur's bound and furthermore that the energy fluctuations are highly damped around the average. We also use this protocol to construct a heat engine which operates in finite time with positive power output and efficiency close to the Carnot efficiency.

We contrast this with the continuous protocol and find that the continuous protocol is unable to reset close to Landauer's bound. We also demonstrate that the fluctuations in the continuous protocol transition between exponentially suppressed in the short time limit to a $1/\tau$ suppression for long times.

In Chapter 3 we present some initial findings about the suitability of experiments on the fluorescence of organic molecules as a test bed for quantum thermodynamics. We show that the Jarzynski relation is satisfied for this system, and discuss a method of combining fluorescence data with the relation to perform spectroscopy. Finally we discuss some future directions for the experiment to take.

2

Extending Landauer's Principle to Finite Time Domains

2.1 Introduction

This chapter is based on the paper [56], which we authored during our postgraduate studies. Landauer's principle [34, 38, 57] states that resetting a bit or qubit in the presence of a heat bath at temperature T costs at least $k_{\mathrm{B}}T\ln 2$ of work, which is dissipated as heat. It represents the fundamental limit to heat generation in (irreversible) computers, which is extrapolated to be reached around 2035 [58].

The principle is also a focal point of discussions concerning how thermodynamics

of quantum and nano-scale systems should be formulated. Of particular interest to us here is the single-shot approach to statistical mechanics [14, 15, 16, 59]. This concerns statements regarding what is guaranteed to happen or not in any single run of an experiment, as opposed to what happens on average. This distinction is important for example in nano-scale computer components, in which large heat dissipations in individual runs of the protocol could cause thermal damage, even if the average dissipation is moderate.

In [59] Landauer's principle was assumed to hold in the strict sense that one can reset a uniformly random qubit at the exact work cost of $k_{\mathrm{B}}T\ln 2$ each run of an experiment. This assumption can be showed to be justified if one allows quasistatic protocols [14, 16].

Real experiments take place in finite time [9, 52, 53, 54, 55, 60, 61, 62, 63, 64]. This chapter is motivated by the concern that fluctuations might be much greater in finite time scenarios, and that the single-shot optimality expressions to date may therefore not be physically relevant. Therefore we extend the protocol for bit reset used in [59] to the finite time regime and analyse what changes. In this regime thermalisation is imperfect, and the quantum adiabatic theorem fails so that one cannot a priori assume that shifting energy levels does not change occupation probabilities. Moreover there are correlations between occupation probabilities at different times.

2.2 Performing a Quasistatic Bit Reset

We examine a simple two-level system, with access to a heat bath and a work reservoir, which we will manipulate with a time-varying Hamiltonian in the regime as set out by [32] and detailed below. This system is exactly equivalent to a (qu)bit. The evolution of the system takes place through two mechanisms [32] (see also [16, 65]):

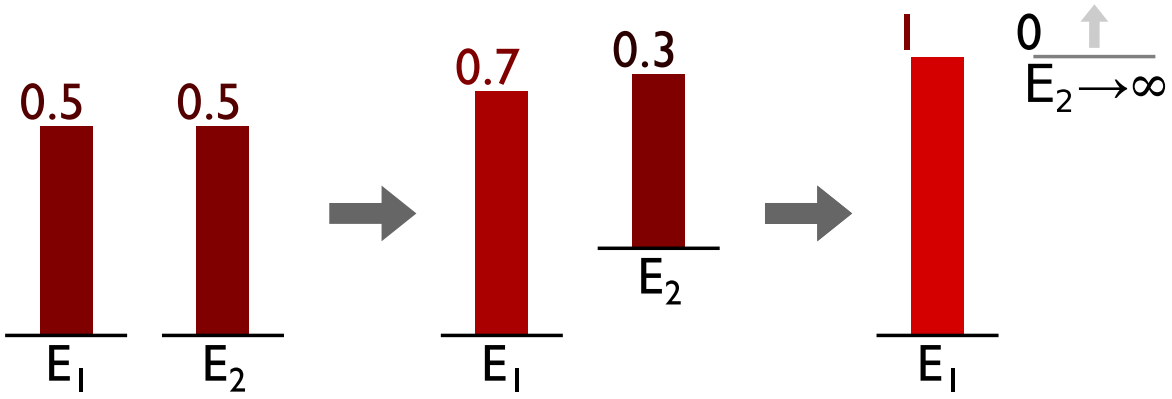


Figure 2.1: **'Bit reset' by raising E_2 to infinity.** *The numbers indicate the occupation probability for the energy levels. We consider the extension of this protocol, running in finite time.*

1. Changes to the energy spectrum – identified with work cost/production $\mathrm{d}E_i$ for occupied energy level i, which has no effect on the occupation probabilities.

2. Changes to probability distributions via interactions with a heat bath (thermalisation), with no changes to the energy spectrum, and thus no associated work cost/production.

Initially, the two degenerate energy levels of a random qubit are equally likely to be populated. The system is coupled to a heat bath at temperature T, and one energy level is quasistatically and isothermally raised to infinity, until the lower energy level is definitely populated (see Fig. 2.1). If we want to perform bit reset ("erasure" in Landauer's terminology), the system is then decoupled from the heat bath, and the second energy level is returned to its original value, such that the initial and final energy level configurations are the same, and only the populations have changed.

In the quasistatic limit, each stage of raising the energy level has an average cost of $P_2 \mathrm{d}E$ where P_2 is the (thermal) population of the upper energy level. Thus raising the

second level from 0 to infinity, the work cost of the entire protocol is given by:

$$\begin{aligned}\langle W\rangle &= \int_0^\infty P_2(E)\mathrm{d}E \\ &= \int_0^\infty \frac{\mathrm{e}^{-\beta E}}{1+\mathrm{e}^{-\beta E}}\mathrm{d}E \\ &= k_\mathrm{B}T\ln 2. \end{aligned} \tag{2.1}$$

2.3 Extending the Protocol to Finite Time

If we wish to examine the effect of finite time on the protocol, there are two different modifications to the above mechanisms we can impose. If we perform a change in the energies in finite time then we will develop coherences in the energy eigenbasis. Alternatively we could limit the time spent thermalising to a finite amount so that we are no longer in a thermal state throughout the energy level changes. Both of these effects will lead to an increase in the amount of work required to perform a bit reset.

2.3.1 The Effects of Quantum Coherence

A development of coherences during the level shifts would increase the amount of work that must be invested to perform a reset. For example, suppose the initial state is $\rho_i = p(a)|a\rangle\langle a| + p(b)|b\rangle\langle b|$, where $|a\rangle$, $|b\rangle$ are the energy eigenstates with occupation probabilities $p(a)$, $p(b)$ respectively. Suppose the Hamiltonian changes very quickly and the new energy eigenstates are $|a'\rangle$, $|b'\rangle$. Using the scheme of [66], we perform a projective measurement in the new energy eigenbasis, $|a'\rangle$, $|b'\rangle$ and define the work input of the step as the energy difference between the initial energy eigenstate and

the final. The average work cost can be written as

$$\begin{aligned}\langle W\rangle &= p(b)(p(b\to b')(E'_b-E_b)+p(b\to a')(-E_b))\\ &+ p(a)(p(a\to a')(0)+p(a\to b')(E_{b'}))\\ &= p(b)(E'_b-E_b)+(p(a)-p(b))p(a\to b')E_{b'},\end{aligned}\tag{2.2}$$

where E_i is the energy of associated with state i, and $p(a\to b')$ indicates the probability of transitioning from a to b'. (In our protocol $E_a{=}E_{a'}{=}0$, and the second line follows by noting that the transition probabilities are doubly-stochastic due to the Born rule). Since $E_{b'}>E_b\geq 0$, and $p(a)\geq p(b)$, in order for this expression to contribute the least work cost possible, we set the transition probability $p(a\to b')$ to zero, i.e. by not causing any coherent excitations.

We therefore avoid coherence, using either one of two ways: (i) By allowing for the experimenter to choose a path of Hamiltonians that share the same energy eigenstates and only differ in energy eigenvalues, as in the standard model for Zeeman splitting, (ii) If the experimenter is instead given a fixed Hamiltonian path which is not of this kind, she may actively remove the coherences by an extra unitary being applied. This method of active correction is similar to the strategy employed in super-adiabatic processes [67, 68, 69]. In a super-adiabatic process one invests an extra amount of energy to compensate for the coherences that develop from proceeding non-quasistatically. Here we can perform the same trick of using an extra unitary but instead pay the extra cost by extracting the energy from the coherences that develop so that the overall energy costs are the same. In either case, at any point of the protocol the density matrix of the system will be diagonal in the instantaneous energy eigenbasis. Further discussion can be found in Appendices A.1 and A.2.

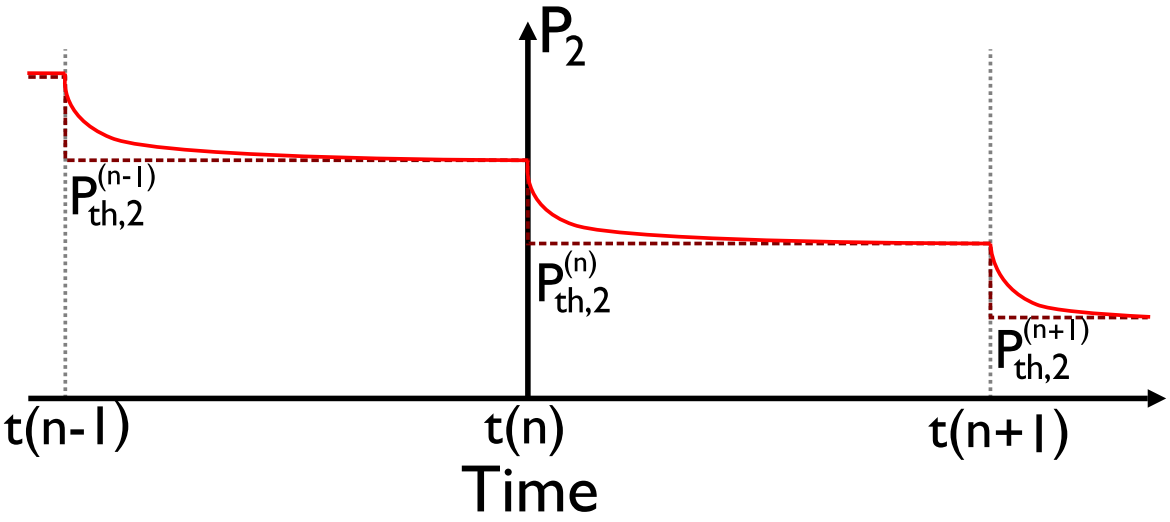


Figure 2.2: **A few steps of the discrete time protocol.** *Thermal (dashed) and actual (solid) upper energy level populations with respect to time. At each time, $t(n)$, the upper energy level is raised, altering the thermal state.*

2.3.2 Partial Thermalisation as a Partial Swap

Consider now the process of thermalisation. At stage n, when the energy levels are split by $\Delta E = n\mathcal{E}$, the associated thermal populations are given by the Gibbs distribution:

$$\mathbf{P}^{\text{th}}(n) = \frac{1}{1+e^{-\beta n\mathcal{E}}} \begin{pmatrix} 1 \\ e^{-\beta n\mathcal{E}} \end{pmatrix}. \tag{2.3}$$

Consider a stochastic transformation in which we have a probability P_{swap} of replacing the current state with the appropriate thermal state, and probability $(1-P_{\text{swap}})$ of leaving the state alone. This is expressed as the stochastic matrix

$$M(n) = (1 - P_{\text{swap}})\ \mathbb{1} + P_{\text{swap}} M_{\text{th}}(n), \tag{2.4}$$

where

$$M_{\text{th}}(n) = \begin{pmatrix} P_1^{\text{th}}(n) & P_1^{\text{th}}(n) \\ P_2^{\text{th}}(n) & P_2^{\text{th}}(n) \end{pmatrix}, \tag{2.5}$$

and $P_i^{\text{th}}(n)$ is the i^{th} component of $\mathbf{P}^{\text{th}}(n)$. We verify that this matrix has the defining behaviour of a thermalising process by considering its eigenvectors, and noting that it evolves all probability distributions towards the thermal distribution.

Under the assumption that we raise the energy levels in such a way that the population of the levels is undisturbed, we can write a recursive relationship between the populations $\mathbf{P}(n)$ at the end of each stage (that is the populations having adjusted the energy level for the n^{th} time, and then allowing it to partially thermalise):

$$\mathbf{P}(n) = \Big(M\,(n)\Big)^{t(n)}\ \mathbf{P}(n-1), \tag{2.6}$$

where $t(n)$ is the number of times we apply the partial thermalisation matrix at stage n.

We attempt instead to express this energy level population as the ideal thermal distribution $\mathbf{P}_{\text{th}}^{(\mathbf{n})}$ perturbed by a small difference,

$$\mathbf{P}(n) \quad = \quad \mathbf{P^{th}}(n) + \boldsymbol{\delta}(n). \tag{2.7}$$

We calculate the correction term $\boldsymbol{\delta}$ explicitly by noting that the probability of not swapping with $\mathbf{P^{th}}(n)$ in any stage is given by $(1 - P_{\text{swap}})^{t(n)}$, and so our correction is to subtract this amount of the thermal population and add instead the same amount of the population of the previous stage:

$$\boldsymbol{\delta}(n) = (1 - P_{\text{swap}})^{t(n)} \Big(-\mathbf{P^{th}}(n) + \mathbf{P}(n-1)\Big)\,. \tag{2.8}$$

We can see that the influence of a finite thermalisation time, t, manifests as a degradation the thermalisation quality through a lowered $P_{\text{sw}}(t)$. Further note that, as $\mathbf{P^{th}}(n)$ and $\mathbf{P}(n)$ are both valid probability distributions, the sum of the components of $\boldsymbol{\delta}$ must sum to zero. This can specifically seen to be the case here by noting that

the second component of each contributing part of $\boldsymbol{\delta}$ is just just one minus the first component. Indeed for a two level system, we can express $\boldsymbol{\delta}$ as:

$$\boldsymbol{\delta}(n) = \pm\delta(n) \begin{pmatrix} 1 \\ \\ -1 \end{pmatrix}, \tag{2.9}$$

where δ is a quantity known also as the trace-distance (see e.g. [70]). The sign of δ depends on whether we are raising or lowering the upper energy level. Incomplete thermalisation after raising the upper energy level leaves a higher probability of being in the upper level than the true thermal probability. There is a lower than thermal probability when lowering the upper energy level.

2.4 The Average Work Cost

We are now in a position to calculate the average work cost for performing a bit reset in finite time. In order to do this we first bound the trace-distance so that we have the worst case scenario where the bit is maximally far away from the thermal state. We are then able to use this state to calculate a bound on the average work cost for resetting a bit in finite time. Furthermore, by examining the structure of the thermalisation we can then create a bound on the 'single-shot' work cost. Finally we can also show how the reset error in this protocol is exponentially suppressed.

2.4.1 Bounding the Trace-Distance

It is possible to quantify to what extent the state at the end of a period of thermalisation differs from a thermal state by employing the trace-distance $\delta(\rho, \sigma) := \frac{1}{2}\mathrm{Tr}(\sqrt{(\rho-\sigma)^\dagger(\rho-\sigma)})$ (see e.g. [70]). The trace distance is the maximum probability

of distinguishing between two states given an optimal measurement and thus provides a measure of how similar the states are. We can bound the trace-distance $\delta(n)$ by noting that, since we increase the energy of the second level throughout the protocol, the effect of thermalization is always to increase the occupation probability of the first energy level $P_1^{(n-1)} \geq P_1^{(0)}$. This can be seen from Eq. 2.8. Thus we have:

$$\begin{aligned} \delta(n) &= (1-p)^t \left(\frac{1}{1+\exp\left(-n\beta\mathcal{E}\right)} - P_1^{(n-1)} \right) \\ &\leq (1-p)^t \left(\frac{1}{1+\exp\left(-n\beta\mathcal{E}\right)} - \frac{1}{2} \right). \end{aligned} \tag{2.10}$$

Having derived a bound on the trace-distance we can now write the probability distribution (after some rearranging) as:

$$\mathbf{P}(n) \leq \begin{pmatrix} \left(1+(1-p)^t\right) \dfrac{1}{1+\exp\left(-n\beta\mathcal{E}\right)} - \dfrac{1}{2}(1-p)^t \\ \left(1+(1-p)^t\right) \dfrac{\exp\left(-n\beta\mathcal{E}\right)}{1+\exp\left(-n\beta\mathcal{E}\right)} - \dfrac{1}{2}(1-p)^t \end{pmatrix}. \tag{2.11}$$

2.4.2 Bounding the Average Work Cost

In the worst case scenario, at each stage before raising the energy level, we are exactly δ away from the true thermal population. Raising the energy level by $\mathcal{E}$ at stage n has an associated work cost of $P_2(n)\mathcal{E} = \left(P_2^{\text{th}}(n) + \delta\right)\mathcal{E}$. We can integrate over the entire protocol to find the worst case average work cost. This allows us to construct a bound the work cost for the reset:

$$\begin{aligned} \langle W_{\text{quasi}} \rangle \leq \langle W \rangle \leq \; & \langle W_{\text{quasi}} \rangle + \\ & (1-p)^t \left(\frac{E_{\max}}{2} - \langle W_{\text{quasi}} \rangle \right). \end{aligned} \tag{2.12}$$

Here we have defined $\langle W_{\text{quasi}} \rangle$ as the quasistatic work cost of raising the sec-

ond level to $E_{\max}$:

$$\langle W_{\text{quasi}} \rangle = k_{\text{B}} T \ln \left(\frac{2}{1 + \exp\left(-\frac{E_{\max}}{k_{\text{B}} T}\right)} \right). \tag{2.13}$$

The physical relevance of this quantity is simply that it denotes the energy that must be required to perform a bit reset quasistatically, up to a certain point - instead of carrying on raising the second energy level to infinity we stop at some finite value. We can see that if $E_{\max} \to \infty$ then $\langle W_{\text{quasi}} \rangle \to k_{\text{B}} T \ln 2$, and we thermalise perfectly ($\delta = 0$), we recover the quasistatic Landauer cost $k_{\text{B}} T \ln 2$ (as derived in Eq. 1). However we can also see that if there is any degree of imperfection in the thermalisation then the work cost of resetting is unboundedly bad due to the non-zero population in the upper energy level throughout the protocol.

2.4.3 Single-Shot Work Cost

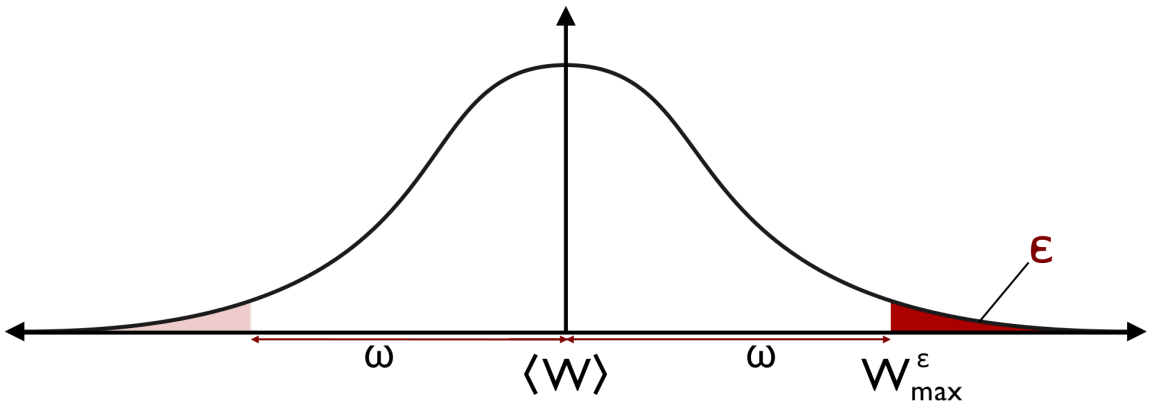


Figure 2.3: **An example probabilistic work distribution.** *Work values are always below $W_{\max}^{\epsilon}$, except with probability of failure ϵ given by the area of the shaded region on the right. The sum of the areas of both the shaded regions on the left and right indicates the probability of failing to be within ω of $\langle W \rangle$ (as given by Eq. 2.15).*

In a single shot classical regime, we assume that at the end of each stage the system

is in one of the two energy levels; and we can express each choice of energy level as a sequence of random variables $\{X_i\}_{i=1\ldots N}$. Noting that at each stage, by raising the splitting of the energy levels by $\mathcal{E}$, if the system is in the upper energy state at a particular stage, then this stage contributes a work cost of $\mathcal{E}$. With this in mind, it is useful to label the two energy levels as 0 or 1 such that the work contribution at each stage is given by $X_i\mathcal{E}$, and thus the *actual work cost* of a bit reset is given by the function acting on the random variables:

$$W(X_1, \ldots, X_N) = \mathcal{E} \sum_{i=1}^{N} X_i. \tag{2.14}$$

It is possible to take the average of this function over some or even all of the random variables. By considering the behaviour of this collection of random variables as detailed in Appendix A.4 we can determine the variation around the average work cost:

$$P(|W - \langle W \rangle| \geq \omega) \;\; \leq \;\; \exp\left(-\frac{2\,\omega^2 {P_{\text{sw}}}^2}{N\mathcal{E}^2}\right). \tag{2.15}$$

This tells us that the probability of the actual work cost W differing from the average $\langle W \rangle$ by an amount greater than some value ω is exponentially suppressed by the square of the minimum difference, the probability of performing a swap and the size of the energy level increments.

2.4.4 Calculating $W^{\epsilon}_{\text{max}}$.

We can express the above result in the language of single-shot statistics by calculating the maximum work, except with some probability of failure ϵ, defined:

$$P(W > W^{\epsilon}_{\text{max}}) := \epsilon, \tag{2.16}$$

We can re-centre this definition around the expectation value of work, $\langle W \rangle$, such that:

$$P\Big(W - \langle W \rangle > W^{\epsilon}_{\max} - \langle W \rangle\Big) = \epsilon, \tag{2.17}$$

and choose $\omega = W^{\epsilon}_{\max} - \langle W \rangle$ (see Figure 2.3). We can combine this with the previously calculated bound on the average work cost for performing a reset to find:

$$\begin{aligned} W^{\epsilon}_{\max} \quad &\leq \quad \langle W_{\text{quasi}} \rangle + \frac{1}{2}(1-p)^t N\mathcal{E} \\ &+ \quad \frac{1}{1-(1-p)^t}\sqrt{\frac{\ln(2/\epsilon)}{2N}}N\mathcal{E}. \end{aligned} \tag{2.18}$$

Firstly, we can see that if we do not thermalise at all (I.E. we take $t \to 0$) then the bound reads $W^{\epsilon}_{\max} \leq \infty$, telling us that there is some probability we need to invest an infinite amount of energy to perform a reset. This arises due to the non-zero occupation of the second energy level and agrees with our physical intuition about the situation. If we take the other extreme and consider allowing an infinite amount of thermalisation time (I.E. taking $t \to \infty$) the situation is not quite as clear. We find that $W^{\epsilon}_{\max} \leq \langle W_{\text{quasi}} \rangle + N\mathcal{E}\sqrt{\frac{\ln(2/\epsilon)}{2N}}$. This quantifies the variation in energy that must be invested due to the fact that we only raise the second energy level to some finite value. Finally, in the interim scenario there is a further contribution due to the incomplete thermalisation of the system which also acts to reduce the impact of the partial raising.

2.4.5 Reset Error is Exponentially Suppressed

In [59] the general protocol involves resetting n qubits in the state $\rho = \mathbb{1}/2 \otimes \mathbb{1}/2 \cdots \otimes \mathbb{1}/2$ and we now consider how the errors scale in this case.

Recall that for a single qubit, thermalising for time t bounds the trace-distance δ between the actual state and the true thermal state according to Eq. 2.10. This

results in an additional work cost of up to $\delta E_{\max}$ across the protocol. For n bits, in the very worst case each bit will be δ away from its thermal state, and so trivially the extra work cost will be bounded by $n\delta E_{\max}$. Thus the average work cost of reset scales linearly with the number of bits (as with the quasistatic case).

This argument can be naturally modified to the single-shot case by noting that our calculated $W^{\epsilon}_{\max}$ has failure probability upper bounded by ϵ, such that $P(W > W^{\epsilon}_{\max}) \leq \epsilon$. For n random bits, the probability that every bit resets under this limit is given by $(1-\epsilon)^n$, such that we can bound:

$$P(W_{\text{tot}} > nW^{\epsilon}_{\text{tot}}) \leq 1 - (1-\epsilon)^n \leq n\epsilon, \tag{2.19}$$

where the final inequality can be proved by induction.

In the worst case scenario, the failure of a single bit to reset under $W^{\epsilon}_{\max}$ causes the entire protocol to fail. We can thus write a bound on the work cost of resetting n bits as $\mathcal{W}^{\epsilon'}_{\max} \leq nW^{\epsilon}_{\max}$ where $\epsilon' = 1-(1-\epsilon)^n$, and as $\epsilon' \leq n\epsilon$ it follows that $\mathcal{W}^{n\epsilon} \leq nW^{\epsilon}_{\max}$. Hence, when resetting $H_{\max}$ bits:

$$\mathcal{W}^{H_{\max}\epsilon} \leq H_{\max} W^{\epsilon}_{\max}. \tag{2.20}$$

Based on this argument we can thus state that the multi-qubit statements in [15, 59] also remain relevant in the case of finite time.

2.5 A Two Level Engine in Finite Time

Although we have thus far concentrated on bit reset, it is also possible to consider the inverse protocol: work extraction by lowering the upper energy level in contact with a hot bath.

2.5.1 Work Extractable in Finite Time

The derivation of this proceeds exactly as before, with the limits of the integration reversed. This allows us to extract work bounded by:

$$\begin{aligned} -\langle W_{\text{quasi}}\rangle &\leq \langle W_{out}\rangle \\ &\leq -\langle W_{\text{quasi}}\rangle + \\ &\quad (1-p)^t \left(\frac{E_{\max}}{2} - \langle W_{\text{quasi}}\rangle\right). \end{aligned} \tag{2.21}$$

If we have access to two baths at different temperatures, we can extract net work by running a bit reset coupled to a cold bath at temperature T_C followed by a work extraction coupled to a hot bath at temperature T_H. The engine cycle formed (shown in Fig. 2.4) has net work exchange per cycle bounded by

$$\begin{aligned} \langle W_{\text{net}}\rangle &\leq -P_{sw}(t)k_{\text{B}}\left(T_H - T_C\right)\ln 2 \\ &\quad -P_{sw}(t)k_{\text{B}}\left(T_C \ln\left(Z_C^{\max}\right) + T_H \ln\left(Z_H^{\max}\right)\right) \\ &\quad + \left(1 - P_{sw}(t)\right)E_{\max}, \\ &= P_{sw}(t)\langle W_{\text{quasi}}\rangle + \left(1 - P_{sw}(t)\right)E_{\max}, \end{aligned} \tag{2.22}$$

where $Z_{C/H}^{max} = 1 + \exp\left(-E_{\max}/k_{\text{B}}T_{C/H}\right)$ and $\langle W_{net}\rangle$ is the difference between the work input (Eq. 2.12) and the work output (Eq. 2.21) with the appropriate temperatures.

The final line follows because the first two lines are the same as in the quasistatic case. The final term is independent of the temperatures of the baths; but instead accounts for the effect of finite time on the degree of over-population of the upper level when raising, and under-population of the upper level when lowering.

Adjusting the energy level in finite steps has necessitated a move away from the truly

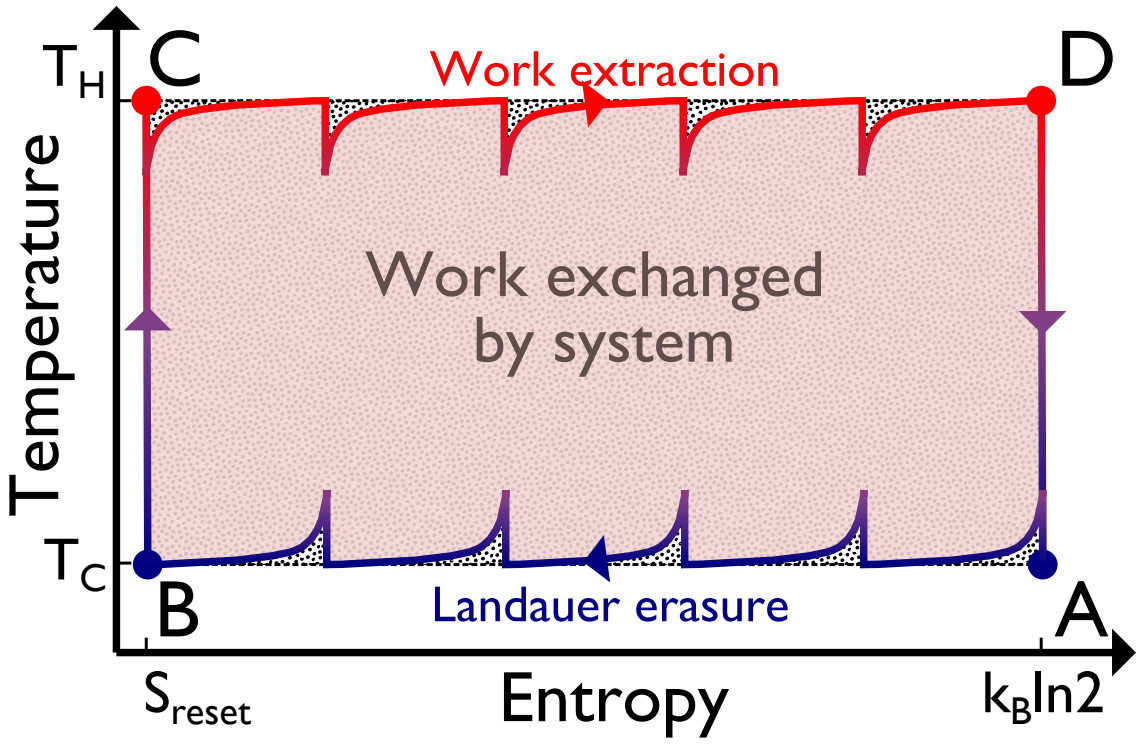


Figure 2.4: **Entropy-temperature diagram for the engine cycle.** *The block shaded area shows the net work exchanged by the system, which is less than that of the quasistatic (Carnot) cycle shown by the dashed rectangle filled with dots behind. For illustrative purposes, the number of energy level adjustments has been greatly reduced, and size of the associated shifts in temperature greatly exaggerated.*

isothermal process of the quasistatic regime. In a two-level system, any distribution where the lower energy level is more populated than the upper may be written as a thermal state for some temperature. During bit reset, after the upper energy level is raised, it is over-populated with respect to the thermal population associated with the cold bath temperature. We can interpret this as a rise in the system temperature appearing as the saw-tooth pattern in Fig. 2.4.

2.5.2 Speed Limit for Positive Power Output

By reconciling the concept of time with these processes, we can now talk meaningfully about the *power* of the cycle, $\mathcal{P}$: the net work exchange divided by the total time

taken to complete a full cycle of bit reset and extraction. The total time is found by multiplying the amount of time spent thermalising in one stage, t, by the number of stages in both halves of the protocol, $N = 2E_{\max}/\mathcal{E}$. We can upper bound the power of the entire cycle as a function of the maximum energy gap $E_{\max}$ and of t:

$$\mathcal{P} \leq \frac{P_{sw}(t)\langle W_{\text{quasi}}\rangle + (1 - P_{sw}(t))\, E_{\max}}{2\dfrac{E_{\max}}{\mathcal{E}}t}. \tag{2.23}$$

A positive $\mathcal{P}$ indicates the system will draw energy in from its surroundings, and therefore we note that the engine does not produce work in all parameter regimes. If one attempts to operates an engine (with $\langle W_{\text{quasi}}\rangle < 0$) quicker than the limit

$$t < \frac{-1}{\ln(1-p)} \ln\left(1 - \frac{E_{\max}}{\langle W^{\text{net}}_{\text{quasi}}\rangle}\right), \tag{2.24}$$

then the partial thermalisation can potentially contribute an excess work cost greater than the engine's quasistatic work output.

2.5.3 Near-Carnot Efficiency in Finite Time

The efficiency η of a cycle may be defined as the net work extracted divided by the maximum work value of one bit of information ($-k_{\text{B}}T_H \ln 2$). We write this as

$$\eta_{\text{quasi}} - \frac{(1-p)^t E_{\max}}{k_{\text{B}}T_H \ln 2} \quad \leq \eta \leq \quad \eta_{\text{quasi}}, \tag{2.25}$$

where η_{quasi} is the quasistatic efficiency of raising to $E_{\max}$ over an infinitely long time, and can be related to the Carnot efficiency η_{C} by

$$\eta_{\text{quasi}} = \eta_{\text{C}} - \frac{\ln\left(Z_H^{\max}\right) - \dfrac{T_C}{T_H}\ln\left(Z_C^{\max}\right)}{\ln 2}. \tag{2.26}$$

Here we are comparing to the Carnot efficiency as this is the efficiency of an engine formed using the standard Landauer reset and work extraction. We see that if t is small, the cost of raising the populated upper energy level takes its toll on the efficiency, potentially plunging it into negative values (work loss) when t does not satisfy Eq. 2.24. Conversely, as $t \to \infty$, the process is maximally efficient, but has no power.

2.6 A Continuous Time Protocol

It may be wondered how many of these results are dependent upon the discrete time protocol where we perform each aspect of the reset separately. To this end let us examine a continuous time version of the same protocol. As a starting of point, the original protocol consists of two ingredients – we perform discrete changes to the Hamiltonian. To convert this to a continuous time protocol we take the limit of when each time step becomes infinitesimally small as detailed in Appendix A.6. We find that the governing equations for the occupation probabilities of each energy level are given by:

$$\frac{\mathrm{d}}{\mathrm{d}t}\begin{pmatrix} p_1 \\ \\ p_2 \end{pmatrix} = -\gamma \begin{pmatrix} p_1 - \frac{1}{Z(t)} \\ \\ p_2 - \frac{\mathrm{e}^{-\frac{\beta E_{\max}}{\tau}t}}{Z(t)} \end{pmatrix}. \tag{2.27}$$

Despite their simple form these equations do not have simple solutions. By using Mathematica we find that they admit hypergeometric functions as their solutions, reproduced here for completeness:

$$\begin{aligned} p_2(t) = \frac{1}{2}\mathrm{e}^{-\gamma t} \quad &+ \quad \frac{\kappa}{2}\,\psi\left(\frac{\kappa}{2}\right) - \frac{\kappa}{2}\psi\left(\frac{1}{2}\left(1+\kappa\right)\right) \\ &+ \quad {}_2F_1\left(1,\kappa;1+\kappa;-\mathrm{e}^{-\frac{\kappa}{\gamma}t}\right) \end{aligned} \tag{2.28}$$

where $\kappa = \gamma\tau/\beta E_{\max}$, $\psi(z)$ is the polygamma function (see [71]) and ${}_2F_1(a,b;c;z)$

is the hypergeometric function (see [72]). These functions are not easy to use in further calculations to determine things like the average work cost, nor do they lend themselves well to developing an intuitive sense of what the mathematics represents in terms of the system behaviour.

Since $p_1 + p_2 = 1$ we focus on the evolution of p_2 as it contributes to the cost of performing a reset, and we proceed by bounding the evolution of the probability distribution using the fact that $1 \leq Z(t) \leq 2$ so that we have:

$$-\gamma\left(p_2 - \frac{1}{2}\mathrm{e}^{\frac{\beta E_{\max}}{\tau}t}\right) \leq p_2(t) \leq -\gamma\left(p_2 - \mathrm{e}^{\frac{\beta E_{\max}}{\tau}t}\right) \tag{2.29}$$

Solving this we find:

$$\begin{aligned} p_2^{\text{lower}}(t) &\geq \frac{\kappa+1}{2(\kappa-1)}\mathrm{e}^{-\gamma t} - \frac{\kappa}{2(\kappa-1)}\mathrm{e}^{-\frac{\gamma}{\kappa}t}, \\ p_2^{\text{upper}}(t) &\leq \frac{2\kappa+1}{2(\kappa-1)}\mathrm{e}^{-\gamma t} - \frac{\kappa}{(\kappa-1)}\mathrm{e}^{-\frac{\gamma}{\kappa}t}, \end{aligned} \tag{2.30}$$

where we have written $\kappa = \gamma\tau/\beta E_{\max}$ as before for ease of notation. We can now calculate bounds on the average work cost for performing a reset. As in the discrete time process, the average work cost is given by:

$$\langle W\rangle = \int_0^{E_{\max}} p_2(t)\mathrm{d}E_1 = -\frac{\gamma}{\kappa}\int_0^{\tau} p_2(t)\mathrm{d}t$$

To aid legibility we split the upper and lower bounds to the average work:

$$\begin{aligned} \langle W_{\text{lower}}\rangle &\geq -\frac{\gamma}{\kappa}\int_0^{\tau} p_2^{lower}(t)\mathrm{d}t \\ &\geq \frac{\gamma\tau+\beta E_{\max}}{\gamma\tau-\beta E_{\max}}\frac{\beta E_{\max}}{2\gamma\tau}\left(\mathrm{e}^{-\gamma\tau}-1\right) + \frac{\gamma\tau}{2\left(\gamma\tau-\beta E_{\max}\right)}\left(1-\mathrm{e}^{-\beta E_{\max}}\right) \end{aligned} \tag{2.31}$$

$$\begin{aligned}\langle W_{\text{upper}}\rangle &\leq -\frac{\gamma}{\kappa}\int_0^\tau p_2^{upper}(t)\mathrm{d}t \\ &\leq \frac{2\gamma\tau+\beta E_{\max}}{\gamma\tau-\beta E_{\max}}\frac{\beta E_{\max}}{2\gamma\tau}\left(\mathrm{e}^{-\gamma\tau}-1\right)+\frac{\gamma\tau}{\gamma\tau-\beta E_{\max}}\left(1-\mathrm{e}^{-\beta E_{\max}}\right) \quad (2.32)\end{aligned}$$

Here we have explicitly written out the dependence of the bounds on the rate of thermalisation γ, the total protocol time τ, the inverse bath temperature β, and the maximum energy of the second energy level $E_{\max}$. Note that even in situation where we let $\gamma, \tau, E_{\max} \to \infty$ we do not recover the quasistatic results. There are multiple explanations for this – the first being that one of the underlying assumptions in our setup has been broken. These equations were derived in the limit of slow thermalisation compared to the time scale of the energy level change – when these become comparable our simplified rate equations for the probability distributions are no longer true. Furthermore, we note that in the discrete protocol it is always possible to allow the probability distribution to relax to the 'right' thermal state before carrying out the energy level shift. When we perform both simultaneously this luxury is no longer afforded to us and we must continuously pay the cost for not being in a true thermal state. Finally we note that these bounds are unfortunately not tight throughout the protocol due to the simplifying assumption of characterising the partition function by its initial and final values.

We would also like to briefly discuss the behaviour of these bounds for long times τ. We can see that in the first term, the exponential component decays leaving the $1/\tau$ behaviour to dominate plus an approximately constant term determined by the energy splitting of the final system. That is our bounds reduce to something of the form $\langle W\rangle \leq k_1 - \frac{k_2}{\tau}$, where k_i are roughly constant.

It is possible to construct an engine by combining a work extraction protocol coupled to a hot bath and a resetting protocol coupled to a cold bath, but the resulting

net work does not have a concise expression as it cannot be expressed in terms of the quasistatic work, nor does it reduce to the quasistatic value in the long time limit. Furthermore, although such an engine can be operated at positive power it is not close to the Carnot efficiency due to irreversible work generated throughout the cycle.

2.6.1 Bounding the Single-Shot Work Cost

We can no longer employ the powerful McDiarmid's inequality due to the system evolving continuously such that we cannot represent the work as a sum of random variables [73]. This prevents us from expressing the work as a Doob martingale and hence we do not satisfy the conditions necessary to use McDiarmid's inequality. Indeed, this difficulty forces us to use the simplest of these concentration of measure bounds – Markov's inequality [74]. The only requirements for Markov's inequality are that the random variable under consideration is non-negative, which by construction our random work variable satisfies. Markov's inequality states that:

$$P(X \geq \alpha) \leq \frac{\langle X \rangle}{\alpha} \tag{2.33}$$

Since we have derived the work as an integral over random variables, it too is a random variable and thus we can employ this simpler bound. By choosing $\alpha = W^{\epsilon}$ such that $P(W \geq W^{\epsilon}) = \epsilon$ we find that:

$$W^{\epsilon} \leq \frac{\langle W \rangle}{\epsilon}. \tag{2.34}$$

Since we have a lower bound on the expected work cost we can find a relatively

tight bound on the single-shot work:

$$W^{\epsilon} \leq \frac{\gamma\tau + \beta E_{\max}}{\gamma\tau - \beta E_{\max}} \frac{\beta E_{\max}}{2\gamma\tau} \frac{\mathrm{e}^{-\gamma\tau} - 1}{\epsilon} + \frac{\gamma\tau}{2\left(\gamma\tau - \beta E_{\max}\right)} \frac{1 - \mathrm{e}^{-\beta E_{\max}}}{\epsilon}. \tag{2.35}$$

For short times the behaviour is dominated by the exponential term so that the fluctuations in the work cost are highly suppressed such that the average cost is a good indicator of the work that must be invested. Using the same arguments as before, we can see that for long times the bound on the fluctuations is approximated by something of the form $W^{\epsilon} \leq \frac{1}{\epsilon}\left(k_1 - \frac{k_2}{\tau}\right)$. This indicates that as the protocol is performed for longer we increase the average quality of the reset as the thermalisation is more complete but admit larger fluctuations to the overall work cost.

2.7 Conclusion

We have shown two protocols, both of which perform the task of resetting a qubit in finite time – albeit with different work costs. If it is possible to isolate the bit being reset such that the two components (thermalisation and energy level changes) can be performed independently of each other then we see that there is a guaranteed work cost of $k_{\mathrm{B}}T\ln 2$ up to some errors that fall off dramatically in the time taken for the protocol. However if both must be performed concurrently then the work cost is linearly bounded by the maximum energy of the second energy level.

As mentioned, several key results in single-shot statistical mechanics assume that this can be achieved perfectly [14, 15, 16, 59, 75]. This work accordingly shows that the optimality statements of those papers are still relevant to finite time protocols. Moreover our results for the discrete time protocol naturally extended to show that the Carnot efficiency can be achieved by a qubit engine in finite time up to an error that

falls of exponentially in the cycle time. Finally we have demonstrated how fluctuations are suppressed in both of these protocols, were we again find a much stronger restriction for the protocol which isolates each component of the reset.

3

Organic Molecules as an Experimental Testbed for Quantum Thermodynamics

3.1 Introduction

The work presented in this chapter is a more detailed examination of that presented in [76]. The theoretical discussions are the author's own work, and we thank Tristan Farrow for carrying out the experiment and providing the insight into the practical methodology used. Marrying the language of thermodynamics with quantum phenomena is giving rise to a quantum thermodynamics whose development defines a new frontier where the transfer of energy at the level of individual quantum objects can now be studied.

The success of thermodynamics owes much to being open to experimental testing in a variety of systems [12]. These have included systems operating in the quantum regime and exhibiting features like quantum coherence, such as quantum dots [77]. Here we seek to demonstrate that the fluorescence of organic molecules forms a natural test-bed for these theories. Our result provides an important proof of concept for the validity of quantum thermodynamics in this regime, and opens the door for more advanced tests of the theory.

Non-equilibrium thermodynamics is evolving rapidly, and a key result is the Jarzynski equality [9, 10, 12]. This concerns the probability distribution of work into a driven system in contact with a heat bath. It essentially equates the average of the exponential work with something which is constant regardless of the driving rate. That constant is the exponential of the equilibrium free energy, i.e. the free energy between a thermal state at the initial boundary conditions and at the final respectively. A key use of this equation is to determine the equilibrium free energy difference from non-equilibrium experiments [78, 79, 80]. The equation also holds for quantum systems [66, 81]. One important area within this field, which has received a large amount of recent attention, is the development of experimental techniques and protocols which can test the theoretical predictions [23, 24].

Parallel developments in physical chemistry with the advent of single molecule spectroscopy [82] over the past decade have opened up unprecedented opportunities for the study of single quantum systems. Unlike studies in bulk where spectroscopic signatures are washed out by the averaging effect of ensembles, these novel techniques now allow individual molecules to be identified, tracked and probed. Thus it is becoming possible to study energy transfers at the level of single molecules, some of which offer

ideal test-beds owing to their well-defined spectroscopic signatures and quantum state dynamics. Their properties are extremely reproducible, more so than rival quantum systems such as quantum dots and nanocrystals [82].

In this work we connect these two approaches, namely quantum thermodynamics and molecular spectroscopy. We consider the spontaneous emission of photons from a single excited organic molecule as a thermodynamic process. We determine the probability distribution of work and heat in the experiment, see 3.3, and find that it satisfies the quantum Jarzynski relation. A key point is to treat the free space around the molecule as an extremely low excitation heat bath, and the fluorescent light as heat transferred into that environment. By combining this with the observed change in internal energy we are able to calculate the amount of work invested along each trajectory. The laser applied initially corresponds to the driving force, as depicted in Fig. 3.3. In the theoretical analysis we use quantum jumps. The core concept in the quantum jump formalism is that the system always occupies a distinct state that undergoes a stochastic evolution which enables it to transition between different energy levels [77, 83] as illustrated in Figs. 3.1 and 3.4. Furthermore, we demonstrate how use of the quantum Jarzynski equality can be used to infer absolute energy-level shifts in molecules from the emitted photons, as opposed to just the relative shift. We thus establish that these organic molecules are a natural and powerful test-bed for non-equilibrium thermodynamics and suggest how they have use in the enhanced detection of force fields.

3.2 Fluctuation Relations for Two-Level Molecule

Consider a two level system, initially in a thermal state with energies E_g and E_e. We send a laser pulse into the system which swaps the occupation probabilities and then wait for it to spontaneously decay. This takes it back to the ground state. We define

the energy provided by the laser to swap the occupation probabilities as work and then the photons released by the molecule as it spontaneously decays as heat.

We can write this as 4 different trajectories, each with their own associated probabilities and energetics. Note we have defined $\Delta E = E_e - E_g$.

We divide the trajectories of the system into these components:

A. Initial state

B. State after being pulsed with laser

C. State after time period for spontaneous decay

We define the energy supplied by the laser in going from **A** to **B** as the work W, the energy emitted by the molecule in transition from **B** to **C** as heat Q and track the total internal energy change ΔU from **A** to **C**.

Traj	**A**	**B**	**C**	W	Q	ΔU
1	$\|g\rangle$	$\|e\rangle$	$\|g\rangle$	ΔE	$-\Delta E$	0
2	$\|g\rangle$	$\|e\rangle$	$\|e\rangle$	ΔE	0	ΔE
3	$\|e\rangle$	$\|g\rangle$	$\|g\rangle$	$-\Delta E$	0	$-\Delta E$
4	$\|e\rangle$	$\|g\rangle$	$\|e\rangle$	$-\Delta E$	ΔE	0

Table 3.1: *Possible trajectories of the system state*

Now we wish to calculate if the Jarzynski relation for work (see Eqs 3.1) holdw for this system:

$$\langle \mathrm{e}^{-\beta(W-\Delta F)} \rangle = 1, \tag{3.1}$$

$$\langle \mathrm{e}^{-\beta(\Delta U-Q)} \rangle = \mathrm{e}^{-\beta \Delta F}. \tag{3.2}$$

The second line arises through the use of the first law to rewrite the work as the difference between the change in internal energy and the heat emitted. To do this

we need to assign probabilities to the different trajectories and calculate the work and heat probability distributions by summing up the trajectories that correspond to a particular value of work or heat. We also note that in this configuration the equilibrium free energy change of the system $\Delta F = 0$.

Trajectory	**Probability**
1	$P(\|g\rangle) P(\|e\rangle \to \|g\rangle)$
2	$P(\|g\rangle) P(\|e\rangle \to \|e\rangle)$
3	$P(\|e\rangle) P(\|g\rangle \to \|g\rangle)$
4	$P(\|e\rangle) P(\|g\rangle \to \|e\rangle)$

Table 3.2: *Probability associated with each trajectory*

Using this information we can calculate the values of $P(W = \Delta E)$ and $P(W = -\Delta E)$. Note that we use the standard definition of $Z = \sum \mathrm{e}^{-\beta E_i}$.

$$\begin{aligned} P(W = \Delta E) &= P(\text{Traj 1}) + P(\text{Traj 2}) \\ &= P(|g\rangle)\left(P(|e\rangle \to |g\rangle) + P(|e\rangle \to |e\rangle)\right) \\ &= P(|g\rangle) = \frac{\mathrm{e}^{-\beta E_g}}{Z}. \end{aligned} \tag{3.3}$$

$$\begin{aligned} P(W = -\Delta E) &= P(\text{Traj 3}) + P(\text{Traj 4}) \\ &= P(|e\rangle)\left(P(|e\rangle \to |g\rangle) + P(|e\rangle \to |e\rangle)\right) \\ &= P(|e\rangle) = \frac{\mathrm{e}^{-\beta E_e}}{Z}. \end{aligned} \tag{3.4}$$

3.2.1 Jarzynski Work Relation

We can now explicitly calculate the Jarzynski relation for work:

$$\begin{aligned}\langle \mathrm{e}^{-\beta W}\rangle &= \frac{\mathrm{e}^{-\beta E_g}}{Z}\mathrm{e}^{-\beta\Delta E} + \frac{\mathrm{e}^{-\beta E_e}}{Z}\mathrm{e}^{\beta\Delta E} \\ &= \frac{\mathrm{e}^{-\beta E_e}}{Z} + \frac{\mathrm{e}^{-\beta E_g}}{Z} \\ &= 1. \end{aligned} \tag{3.5}$$

So we can see that the system respects the Jarzynski relation for work. Now if we assume that there is a small error term in the probability for each work value we can calculate the effect it has on the Jarzynski relation for work. Let $P(W = \Delta E) = \frac{\mathrm{e}^{-\beta E_g}}{Z} + \delta$ and $P(W = -\Delta E) = \frac{\mathrm{e}^{-\beta E_e}}{Z} + \delta$. This gives us:

$$\begin{aligned}\langle \mathrm{e}^{-\beta W}\rangle &= \left(\frac{\mathrm{e}^{-\beta E_g}}{Z} + \delta\right)\mathrm{e}^{-\beta\Delta E} + \left(\frac{\mathrm{e}^{-\beta E_e}}{Z} - \delta\right)\mathrm{e}^{\beta\Delta E} \\ &= \frac{\mathrm{e}^{-\beta E_e}}{Z} + \frac{\mathrm{e}^{-\beta E_g}}{Z} - \delta\left(\mathrm{e}^{\beta\Delta E} + \mathrm{e}^{-\beta\Delta E}\right) \\ &= 1 - \frac{\delta}{2}\sinh(\beta\Delta E). \end{aligned} \tag{3.6}$$

There are a few interesting points to note about how the Jarzynski relation is satisfied in this set-up. Firstly, we can see that it should be satisfied for all times during the protocol as the transition probabilities drop out and we only depend on the initial state probabilities. Secondly we note that we do depend on unlikely trajectories being accounted for and measured to have the equation balance correctly. This is of importance as experimentally it is probable that we won't have any statistics for such trajectories making an experimental test of the Jarzynski relation more difficult.

3.2.2 Crooks' Relation

Having established that the system obeys the Jarzynski relations it is interesting to consider if it also obeys the Crooks' relation between forward and reverse trajectories. This relation allows one to use information about a particular trajectory to give a probability of the inverse trajectory occurring. The relation may be stated as:

$$\frac{P(A \to B)}{P(B \to A)} = \mathrm{e}^{\beta W_{A\to B} - \Delta F}. \tag{3.7}$$

where $W_{A\to B}$ is the work required to go from A to B and ΔF is the difference in the equilibrium free energies of A and B. In order to check if this relation holds we need to define the inverse trajectories for the system and assign the correct probabilities to them. These will also have three stages:

A. Initial state

B. State after time period for spontaneous excitation

C. State after laser pulse

We also have to update the definitions of work and heat to correspond to the new processes that cause transitions. Work W is defined as the energy required to go from **B** to **C** and heat Q is the energy involved in transitioning from **A** to **B**. The internal energy change ΔU is still the total energy change along **A** to **C**.

Now we can try computing the Crooks' relation directly for one of the trajectories. Note for this system that $\Delta F = 0$ as the initial and final configurations of the molecule are the same. Picking trajectory 1 we have:

$$\mathrm{e}^{-\beta\Delta E} = \frac{P_{\mathrm{fwd}}(|g\rangle \to |g\rangle)}{P_{\mathrm{inv}}(|g\rangle \to |g\rangle)} = \frac{P(|g\rangle)P(|e\rangle \to |g\rangle)}{P(|g\rangle)P(|g\rangle \to |e\rangle)} = \frac{P(|e\rangle \to |g\rangle)}{P(|g\rangle \to |e\rangle)}. \tag{3.8}$$

Table 3.3: *Table showing the inverse trajectories and their probabilites*

Inverse Traj	**A**	**B**	**C**	W	Q	ΔU	**Probability**
1	$\|g\rangle$	$\|e\rangle$	$\|g\rangle$	$-\Delta E$	ΔE	0	$P(\|g\rangle) P(\|g\rangle \to \|e\rangle)$
2	$\|e\rangle$	$\|e\rangle$	$\|g\rangle$	$-\Delta E$	0	$-\Delta E$	$P(\|e\rangle) P(\|e\rangle \to \|e\rangle)$
3	$\|g\rangle$	$\|g\rangle$	$\|e\rangle$	ΔE	0	ΔE	$P(\|g\rangle) P(\|g\rangle \to \|g\rangle)$
4	$\|e\rangle$	$\|g\rangle$	$\|e\rangle$	ΔE	$-\Delta E$	0	$P(\|e\rangle) P(\|e\rangle \to \|g\rangle)$

This equation is a statement of detailed balance between the probability of spontaneous excitation and spontaneous emission. If this equation is satisfied then the Crooks' relation holds between along the trajectories of the joint system. Here we can see that it is possible to satisfy the Jarzynski relation without satisfying Crooks', as it is a weaker condition on the system.

3.2.3 Using Jarzynski to Measure Energy Shifts

We can utilize the Jarzynski equality to detect shifts in the energy spectra of the molecule. If we consider taking the energy levels from:

$$\begin{aligned} E_1 &\to E_1 + \xi \\ E_2 &\to E_2 + \xi + \epsilon, \end{aligned} \tag{3.9}$$

where ξ is a common shift of the energies and ϵ is the difference in shifts between energy levels 1 and 2. This operation produces a change in the equilibrium free energy ($F = -k_B T \ln Z$) of the molecule:

$$\begin{aligned} \Delta F &= k_{\mathrm{B}} T \ln\left(\frac{Z_f}{Z_i}\right) \\ &= -\xi + k_{\mathrm{B}} T \ln\left(\frac{1+\mathrm{e}^{-\beta\Delta E'}}{1+\mathrm{e}^{-\beta\Delta E}}\right). \end{aligned} \tag{3.10}$$

Here we have defined $\Delta E = E_2 - E_1$ and $\Delta E^{'} = \Delta E + \epsilon$. By observing the fluorescence emitted by the excited molecules we can determine the value of both of these quantities. Combining this relation with the Jarzynski equality for heat we can determine the value of ξ. This would allow for probing the strengths of local field effects with high sensitivity. We have:

$$\begin{aligned} \langle \mathrm{e}^{-\beta W} \rangle &= \mathrm{e}^{-\beta \Delta F} \\ &= \frac{1 + \mathrm{e}^{-\beta \Delta E}}{1 + \mathrm{e}^{-\beta \Delta E'}} \mathrm{e}^{\beta \xi}. \end{aligned} \tag{3.11}$$

3.3 Quantum Jump Model of a Laser-Pumped Two-Level Molecule

3.3.1 With a Mixed Initial State

Consider a two level molecule that is in contact with an environment. Initially the environment has no photons in it. The joint state of the environment and molecule is given by

$$\rho_{\text{initial}} = \beta_i |00\rangle\langle 00| + \alpha_i |10\rangle\langle 10|. \tag{3.12}$$

where $\alpha_i + \beta_i = 1$. We require that the reduced density matrix of the system has a thermal distribution. That is we have:

$$\rho_i^{\text{mol}} = \mathrm{Tr}_{\text{bath}}[\rho_i] = \frac{\mathrm{e}^{-\beta E_0}}{Z} |0\rangle\langle 0|_{\text{mol}} + \frac{\mathrm{e}^{-\beta E_1}}{Z} |1\rangle\langle 1|_{\text{mol}}. \tag{3.13}$$

where as usual we define $Z = \sum \mathrm{e}^{-\beta E_i}$. The joint system undergoes a unitary evolution driven by the laser. The action of the laser is simply to invert the occupation probabilities of the joint states. This takes the state to:

$$\rho_i = \alpha_i |00\rangle\langle 00| + \beta_i |10\rangle\langle 10|. \tag{3.14}$$

The joint system then undergoes unitary evolution governed by some interaction Hamiltonian between the molecule and environment. We choose the action of the unitary so that it performs the following operations:

$$\begin{aligned} |00\rangle &\rightarrow |00\rangle, \\ |01\rangle &\rightarrow \mu|01\rangle + \nu|10\rangle, \\ |10\rangle &\rightarrow \mu^*|10\rangle - \nu^*|01\rangle, \\ |11\rangle &\rightarrow |11\rangle. \end{aligned} \tag{3.15}$$

We impose that $|\mu|^2 + |\nu|^2 = 1$. The corresponding matrix representation of U is:

$$U = \begin{pmatrix} 1 & 0 & 0 & 0 \\ 0 & \mu & -\nu^* & 0 \\ 0 & \nu & \mu^* & 0 \\ 0 & 0 & 0 & 1 \end{pmatrix}. \tag{3.16}$$

This matrix simply performs a partial swap on the state of the molecule and the state of the environment. If we propagate our initial state we find:

$$\rho_i' = \alpha_i |00\rangle\langle 00| + \beta_i \left(|\nu|^2 |01\rangle\langle 01| + |\mu|^2 |10\rangle\langle 10| - \mu\nu^* |10\rangle\langle 01| - \nu\mu^* |01\rangle\langle 10| \right). \tag{3.17}$$

We then perform a measurement of the heat bath state. This has the effect of performing a partial measurement on the state of the molecule due to the correlations that have exist between the molecule and heat bath. The state after measurement is:

$$\begin{aligned}
\rho_i'' &= \frac{(\mathbb{1}_{\text{mol}} \otimes |0\rangle\langle 0|_{\text{bath}})\, \rho_i' \,(\mathbb{1}_{\text{mol}} \otimes |0\rangle\langle 0|_{\text{bath}})}{\text{Tr}[(\mathbb{1}_{\text{mol}} \otimes |0\rangle\langle 0|_{\text{bath}})\, \rho_i']} \\
&= \frac{\left(\alpha_i |0\rangle\langle 0|_{\text{mol}} + \beta_i \,|\mu|^2\, |1\rangle\langle 1|_{\text{mol}}\right)}{\alpha_i + \beta_i |\mu|^2} \otimes |0\rangle\langle 0|_{\text{bath}}, \\
&\text{or} \\
\rho_i'' &= \frac{(\mathbb{1}_{\text{mol}} \otimes |1\rangle\langle 1|_{\text{bath}})\, \rho_i' \,(\mathbb{1}_{\text{mol}} \otimes |1\rangle\langle 1|_{\text{bath}})}{\text{Tr}[(\mathbb{1}_{\text{mol}} \otimes |1\rangle\langle 1|_{\text{bath}})\, \rho_i']} \\
&= |0\rangle\langle 0|_{\text{mol}} \otimes |1\rangle\langle 1|_{\text{bath}}. \qquad (3.18)
\end{aligned}$$

Based on the results of this measurement we can assign probabilities for the addition of 0 or 1 quanta of heat to the environment:

$$\begin{aligned}
P_i(Q=0) &= \alpha_i + \beta_i |\mu|^2, \\
P_i(Q=1) &= \beta_i |\nu|^2. \qquad (3.19)
\end{aligned}$$

Now we assume that the environment is sufficiently large that we can throw away our information about it and couple the molecule to a new environment state with zero photons in it. We define this sequence of operations to be our 'sub-protocol', which by repeating some number m times forms our overall protocol. I.E. we consider the joint state of the molecule and environment to be:

$$\rho_{i+1} = \alpha_{i+1} |00\rangle\langle 00| + \beta_{i+1} |10\rangle\langle 10|. \qquad (3.20)$$

Using this we can define coupled recursion relations for α and β. We have:

$$\begin{aligned} \alpha_{i+1} &= \alpha_i + \beta_i |\nu|^2, \\ \beta_{i+1} &= \beta_i |\mu|^2. \end{aligned} \tag{3.21}$$

We can solve these relations to find the value of α and β for arbitrary n. This gives us:

$$\begin{aligned} \alpha_n &= 1 - \beta_0 |\mu|^{2n}, \\ \beta_n &= \beta_0 |\mu|^{2n}. \end{aligned} \tag{3.22}$$

Now using this we can get an expression for the probability of contributing 0 or 1 heat quanta to the environment during the n^{th} iteration of the sub-protocol. To do this consider the trajectory map:

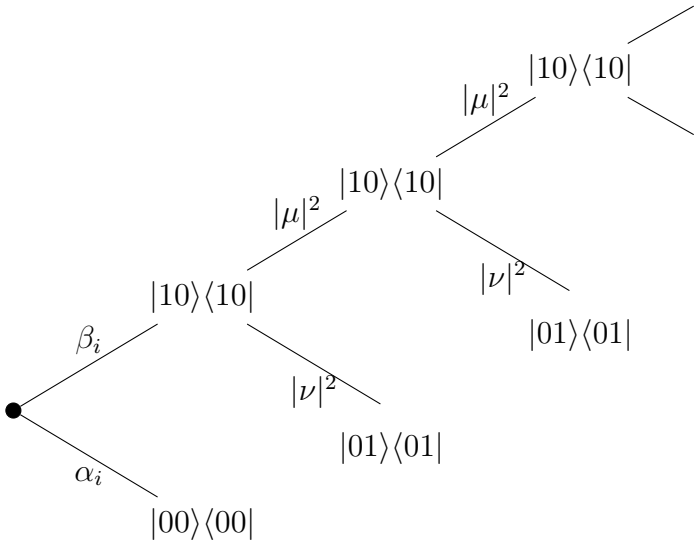


Figure 3.1: A sample of the different trajectories *the system can take after interacting with the environment several times, aftering having been initialized in a mixed state.*

Thus we can see that the probability to have not contributed heat $Q = 1$ to the

environment after some number of steps n is given by:

$$P(Q=0) = \alpha_i + \beta_i |\mu|^{2n}. \tag{3.23}$$

Once the molecule has output one photon of heat to the environment it is no longer able to do so, until it is excited by the laser again. Thus the probability to have contributed heat $Q = 1$ to the environment after n steps is simply:

$$\begin{aligned} P(Q=1) &= 1 - P(Q=0) \\ &= 1 - \alpha_i - \beta_i |\mu|^{2n} \\ &= \beta_i (1 - |\mu|^{2n}). \end{aligned} \tag{3.24}$$

It is possible to map the parameters in this model to the experimental data – in particular there should be some relation between $P(Q=0)$ and the decay curve fit $\mathrm{e}^{-\frac{t}{\tau}}$.

3.3.2 With a Coherent Initial State

Consider a two level molecule that is in contact with an environment. Initially the environment has no photons in it. The joint state of the environment and molecule is given by

$$|\psi\rangle_{\text{initial}} = (\gamma_i |0\rangle + \chi_i |1\rangle) \otimes |0\rangle. \tag{3.25}$$

where $|\chi_i|^2 + |\gamma_i|^2 = 1$.The joint system undergoes a unitary evolution driven by the laser. The action of the laser is simply to invert the occupation probabilities

of the joint states. This takes the state to:

$$|\psi_i\rangle = (\chi_i|0\rangle + \gamma_i|1\rangle) \otimes |0\rangle. \tag{3.26}$$

The joint system then undergoes unitary evolution governed by some interaction Hamiltonian between the molecule and environment. We choose the action of the unitary so that it performs the following operations:

$$\begin{aligned} |00\rangle &\rightarrow \mathrm{e}^{-i\theta}|00\rangle, \\ |01\rangle &\rightarrow \mu|01\rangle + \nu|10\rangle, \\ |10\rangle &\rightarrow \mu^*|10\rangle - \nu^*|01\rangle, \\ |11\rangle &\rightarrow \mathrm{e}^{-i\phi}|11\rangle. \end{aligned} \tag{3.27}$$

We impose that $|\mu|^2 + |\nu|^2 = 1$. The corresponding matrix representation of U is:

$$U = \begin{pmatrix} \mathrm{e}^{-i\theta} & 0 & 0 & 0 \\ 0 & \mu & -\nu^* & 0 \\ 0 & \nu & \mu^* & 0 \\ 0 & 0 & 0 & \mathrm{e}^{-i\phi} \end{pmatrix}. \tag{3.28}$$

This matrix simply performs a coherent partial swap on the state of the molecule and the state of the environment. A unitary operator of this form naturally arises if we model the interaction of the molecule with the environment using a Jaynes-Cummings Hamiltonian. If we propagate our initial state we find:

$$|\psi_i'\rangle = \chi_i \mathrm{e}^{-i\theta}|00\rangle + \gamma_i \left(\mu^*|10\rangle - \nu^*|01\rangle\right). \tag{3.29}$$

We then perform a measurement of the heat bath state. This has the effect of performing a partial measurement on the state of the molecule due to the correlations that have exist between the molecule and heat bath. The state after measurement is:

$$\begin{aligned}
|\psi_i''\rangle &= \frac{(\mathbb{1}_{\text{mol}} \otimes |0\rangle\langle 0|_{\text{bath}})}{\sqrt{\text{Tr}[(\mathbb{1}_{\text{mol}} \otimes |0\rangle\langle 0|_{\text{bath}})\,|\psi_i'\rangle\langle\psi_i'|]}}|\psi_i'\rangle \\
&= \frac{\chi_i \text{e}^{-i\theta}|0\rangle_{\text{mol}} + \gamma_i\mu^*|1\rangle_{\text{mol}}}{\sqrt{|\chi_i|^2 + |\gamma_i|^2|\mu|^2}} \otimes |0\rangle_{\text{bath}}, \\
\text{or} & \\
|\psi_i''\rangle &= \frac{(\mathbb{1}_{\text{mol}} \otimes |1\rangle\langle 1|_{\text{bath}})}{\sqrt{\text{Tr}[(\mathbb{1}_{\text{mol}} \otimes |1\rangle\langle 1|_{\text{bath}})\,|\psi_i'\rangle\langle\psi_i'|]}}|\psi_i'\rangle \\
&= |01\rangle. \qquad (3.30)
\end{aligned}$$

Based on the results of this measurement we can assign probabilities for the addition of 0 or 1 quanta of heat to the environment:

$$\begin{aligned}
P_i(Q=0) &= |\chi_i|^2 + |\gamma_i|^2|\mu|^2, \\
P_i(Q=1) &= |\gamma_i|^2|\nu|^2. \qquad (3.31)
\end{aligned}$$

Now we assume that the environment is sufficiently large that we can throw away our information about it and couple the molecule to a new environment state with zero photons in it. We can view this process as having a destructive measurement of the photon which removes the photon from the system as we detect it. We define this sequence of operations to be our 'sub-protocol', which by repeating some number n times forms our overall protocol. The evolution of the system throughout repeated sub-protocols is best illustrated by using a probability tree once again. This also has the benefit of allowing a direct comparison to the case were we initialize with a mixed state.

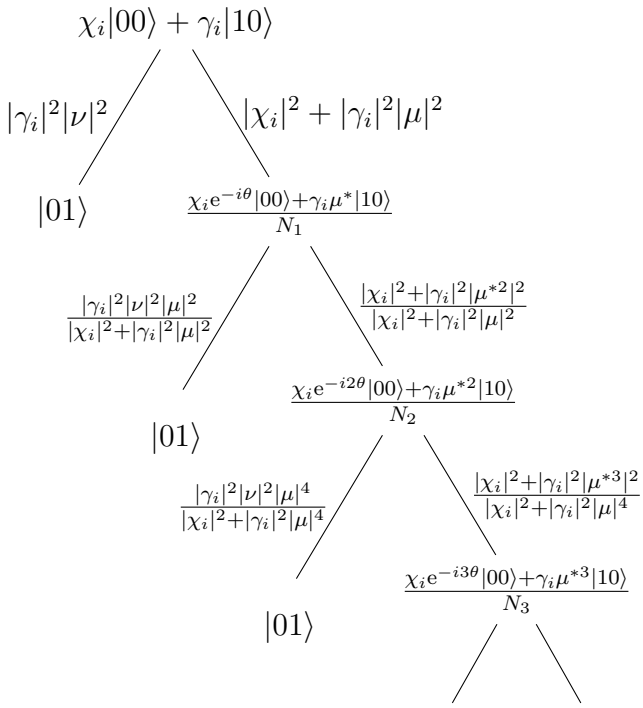


Figure 3.2: A sample of the different trajectories *the system can take after interacting with the environment several times, after having been initialized with a coherent state. The normalization factors, N_i, are simply given by the square root of the probability of each branch.*

We are now in a position to calculate the probability of not transferring a photon of heat into the environment after n sub-protocols, by following the relevant trajectory through the probability tree. Doing so gives us (after simplification):

$$P(Q=0) \;=\; |\chi_i|^2 + |\gamma_i|^2|\mu|^{2n}. \tag{3.32}$$

Once again, after the molecule has transferred a photon of heat to the environment it is no longer able to do so until it is re-excited by the laser. Thus the probability

of having transferred a photon into the environment after n steps is simply:

$$\begin{aligned} P(Q=1) &= 1 - P(Q=0) \\ &= 1 - \left(|\chi_i|^2 + |\gamma_i|^2 |\mu|^{2n}\right) \\ &= |\gamma|^2 \left(1 - |\mu|^{2n}\right). \end{aligned} \tag{3.33}$$

Here we can see that there is no difference in the probability distributions for heat transfer between starting in a mixed state and starting with a coherent state for an appropriate choice of correspondence between β_i and $|\gamma_i|^2$. The lack of a difference between a coherent initial state and the mixed initial state arises due to the choice of basis we perform the measurement in. If we were able to perform a measurement on the output photons in a different basis then we would, in principle, be able to observe a statistical difference between the initial states. This is a potential modification that can be made to the experiment, possibly allowing for investigations into heat statistics with coherences in the bath.

3.4 A Description of the Experiment

The experiment under consideration is the fluorescence of an organic molecule, dibenzoterrylene (DBT), after it is excited via laser pulse. The DBT can be inserted at two sites within the extended anthracene crystal lattice, such that they act as defects and produce two distinct spectral lines at 785nm and 795nm. The blue-shifted site with a transition line of 785nm is the brighter of the two lines so we probed its properties during this study. The full system-environment Hamiltonian is more complicated than necessary for the current investigation so we make some simplifying approximations, as depicted in Fig. 3.3. Despite the relative complexity of the organic molecules, the

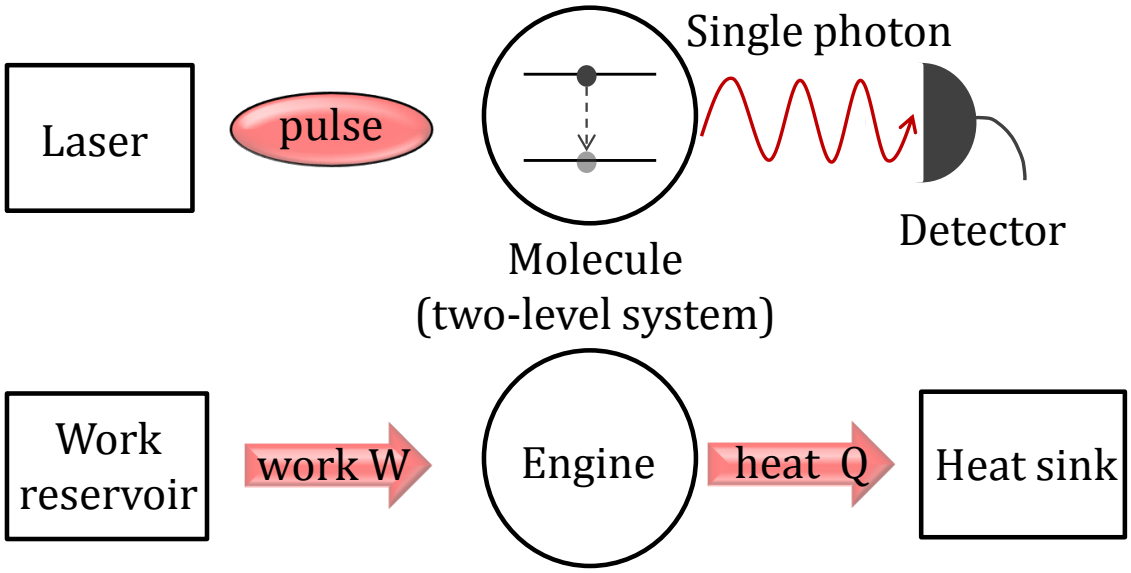


Figure 3.3: Schematic of a two-level molecule *driven by laser pulses generating single photons from decaying electronic states with our thermodynamical representation of the process below it.*

energy level structure of DBT effectively reduces to a that of a two level atom-like state, typical of organic fluorescent dyes. We pumped DBT above resonance to generate excited states that decayed non-radiatively on pico-second timescales into the first excited state $S_{1,0}$. Decay from $S_{1,0}$ into the ground state $S_{0,0}$ gave rise to a sharp lifetime limited line (30Mhz), which, in a single molecule, gives rise to the emission of a single photon for each decay. The narrow width of the Zero Phonon Line (ZPL) is lifetime-limited with a width of approx. 30MHz. These photons emitted from the decay are then captured using time-resolve fluorescence spectroscopy. This gives rise to a waveform which represents a probability distribution of the arrival times of single photons from the decaying state rather than the shape of an optical signal. The time-resolved technique relies on time-correlated single photon counting of pulses obtained by exciting the sample with a 730 nm pulsed laser with a repetition rate of

80MHz. The probability of detecting more than one photon per excitation period is negligible and so we can treat the system as a single photon source. The excited state which gives to the ZPL emission line is found to have a characteristic lifetime of 5ns aftering fitting the exponential decay constant. The experiment under consideration is the fluorescence of an organic molecule (DBT) after it is excited via laser pulse. The DBT can be inserted at two sites within the extended anthracene crystal lattice, such that they act as defects and produce two distinct spectral lines at 785nm and 795nm. The blue-shifted site with a transition line of 785nm is the brighter of the two lines so probe its properties during this study. The full system-environment Hamiltonian is more complicated than necessary for the current investigation so we make some simplifying approximations, as depicted in Fig. 3.3. Despite the relative complexity of the organic molecules, the energy level structure of DBT effectively reduces to a that of a two level atom-like state, typical of organic fluorescent dyes. We pumped DBT above resonance to generate excited states that decayed non-radiatively on pico-second timescales into the first excited state $S_{1,0}$. Decay from $S_{1,0}$ into the ground state $S_{0,0}$ gave rise to a sharp lifetime limited line (30Mhz), which, in a single molecule, gives rise to the emission of a single photon for each decay. The narrow width of the Zero Phonon Line (ZPL) is lifetime-limited with a width of approx. 30MHz. These photons emitted from the decay are then captured using time-resolve fluorescence spectroscopy. This gives rise to a waveform which represents a probability distribution of the arrival times of single photons from the decaying state rather than the shape of an optical signal. The time-resolved technique relies on time-correlated single photon counting of pulses obtained by exciting the sample with a 730 nm pulsed laser with a repetition rate of 80MHz. The probability of detecting more than one photon per excitation period is negligible and so we can treat the system as a single photon source. The excited state which gives to the ZPL emission line is found to have a characteristic

lifetime of 5ns aftering fitting the exponential decay constant.

In summary, we can present the simplified model of the experiment - firstly, we drive the system by using a slightly off-resonance laser (doing work on the system). The system then relaxes non-radiatively to the excited state which then spontaneously emits a photon and decays to the ground state. These photons are emitted to the environment, which we represent as a cold heat bath with zero photons currently in it. We can count these photons as they are emitted to determine the amount of heat being released into the environment and use this to calculate the Jarzynski relation.

3.5 Mapping Experiment to Theory

In order to correctly map the data to our model we must identify which trajectories we observe from Table 3.1. Experimentally we detect clicks in the detector which corresponds to photon emission by the system. An important subtlety is that we only detect a single click even if there are multiple photons emitted. In this analysis we assume that the probability of such an event is sufficiently low so that it is reasonable to ignore it.

Under the experimental scheme we would detect trajectories 1 and 3 as they feature the $|e\rangle \rightarrow |g\rangle$ transition. However, there is a physical difference between these events. The time period for trajectory 3 is substantially shorter than trajectory 1 and is completely subsumed by the photon detectors warm-up period. Hence we do not observe these events, and only observe clicks due to trajectory 1, which has a much longer lifetime. This allows us to map the 'click probability distribution' to the photon probability distribution directly, and thus determine the heat probability distribution.

In order to perform this mapping, we normalize the photon probability distribution by the total number of photons emitted during the active period of the APD (between

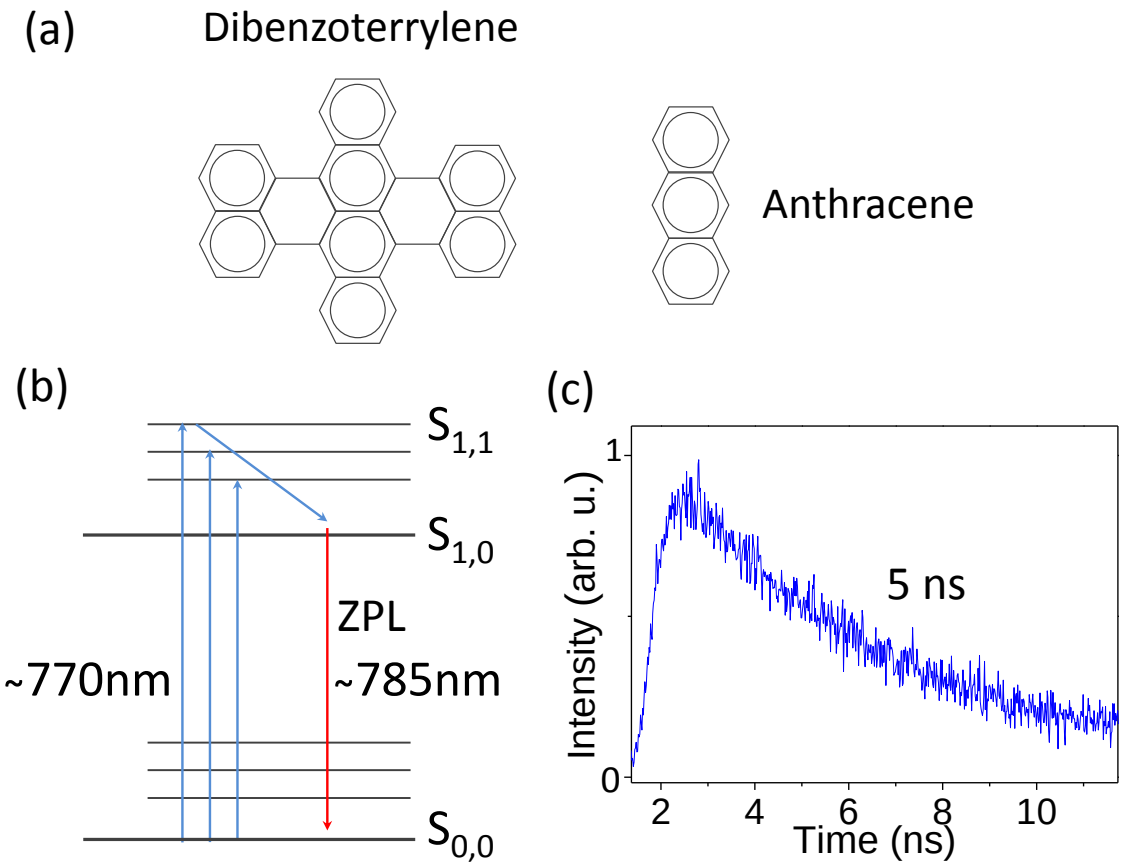


Figure 3.4: ***(a)*** *Dibenzoterrylene (DBT) and anthracene structures consist of corrugated planar assemblies of aromatic hydrocarbons.* ***(b)*** *The energy level structure of DBT* ***(c)*** *Waveform of the decay of excited electronic states in DBT at a temperature of 4K obtained by time-resolved fluorescence spectroscopy. The waveform represents a probability distribution of the arrival times of single photons from the decaying state rather than the shape of an optical signal.*

100,000 and 1,000,000 photons for the range of temperatures). This gives the probability of a photon emission in a particular time bin, and so we simply take the cumulative probability to form the heat probability distribution.

Using this distribution we can then compute the Jarzynski relation for the experimental data. If the relation holds we should find $\langle e^{-\beta(\Delta U - Q)} \rangle = 1$, at all points in the experiment.

The key result of the theoretical model is that the cumulative heat probability

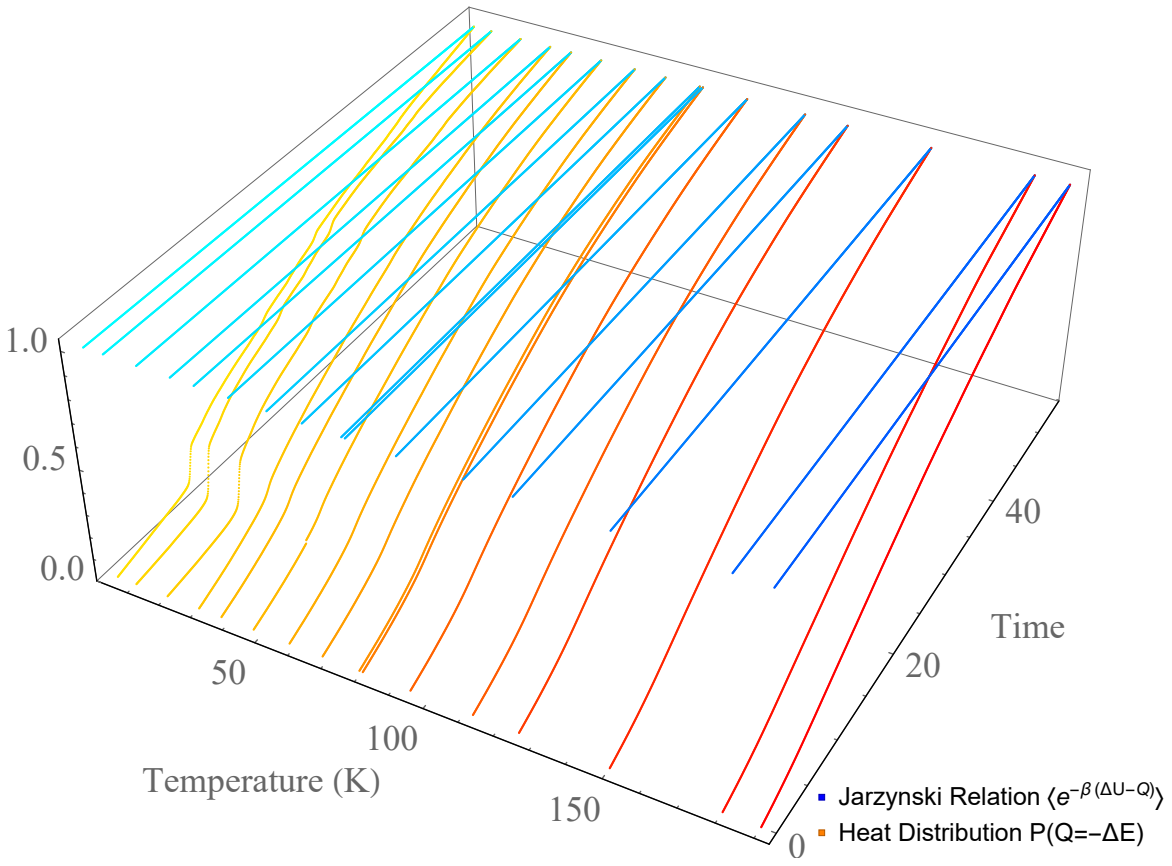


Figure 3.5: Heat distribution and the Jarzynski equality *for an organic molecule undergoing spontaneous emission at a range of different temperatures. The solid curve is the result of overlaying the theoretical prediction of* $\langle \mathrm{e}^{-\beta(\Delta U-Q)}\rangle = 1$ *with the experimentally calculated value. The two results have such close agreement it is not possible to distinguish between them, demonstrating that the Jarzynski equality holds for all times during the emission. The lower dashed curve represents part of the heat distribution, which has been calculated directly from the spectroscopic data. The other component of the heat distribution is simply the reverse of the presented quantity, as can be seen from* $P(Q=-\Delta E)=1-P(Q=\Delta E)$*. This is generated from the spectroscopic data by considering the cumulative number of photons emitted up to a particular time and renormalizing by the total number of photons.*

distribution is given by:

$$P\left(Q=-\Delta E||g\rangle\right)=\beta\left(1-|\mu|^{2n}\right). \tag{3.34}$$

where β is the long time probability of $P\left(Q = -\Delta E||g\rangle\right)$ and $|\mu|^2$ is the swapping parameter.

Thus we have a direct relation between trajectory 1 and the model:

$$P(\text{Traj 1}) = P(|g\rangle)P_{\text{eg}}(n) = \beta(1 - |\mu|^{2n}). \tag{3.35}$$

For long times we expect $P_{\text{eg}} \to 1$ so there is a direct equivalence between $P(|g\rangle)$ and β. Hence $P_{\text{eg}}(n) = 1 - |\mu|^{2n}$ and we can rearrange this equation to make use of the data we have in the form of the time resolved trace. This allows us to plot $|\mu|^2$ against time and determine the average swapping parameter.

We can also consider mapping the model to the exponential decay curve, $P(|e\rangle = P_0 \mathrm{e}^{-\frac{t}{\tau}}$. If we discretize this, using $t = n\Delta t$ then we find:

$$\tau = -\frac{\Delta t}{\ln(|\mu|^2)}. \tag{3.36}$$

The average value of the swapping parameter is confined between $4.3 \leq \langle\tau\rangle \leq 4.7$ ns, which has reasonable agreement with the experimental fit. The difference is most likely due to artifacts from treating time as a discrete parameter in the theoretical analysis.

3.6 Conclusion

We conclude that this fluorescence experiment amounts to a scenario where Jarzynski's equality holds. As further evidence that this experimental set-up is promising for probing quantum thermodynamics we note/reiterate the following: (i) molecular spectroscopy is a powerful and well-established technique, (ii) the set-up maps naturally to the quantum jumps model for work and heat (used e.g. in Crooks' proof of Quantum Jarzynski [10]). Furthermore, we conclude that the Jarzynski relation is satisfied even

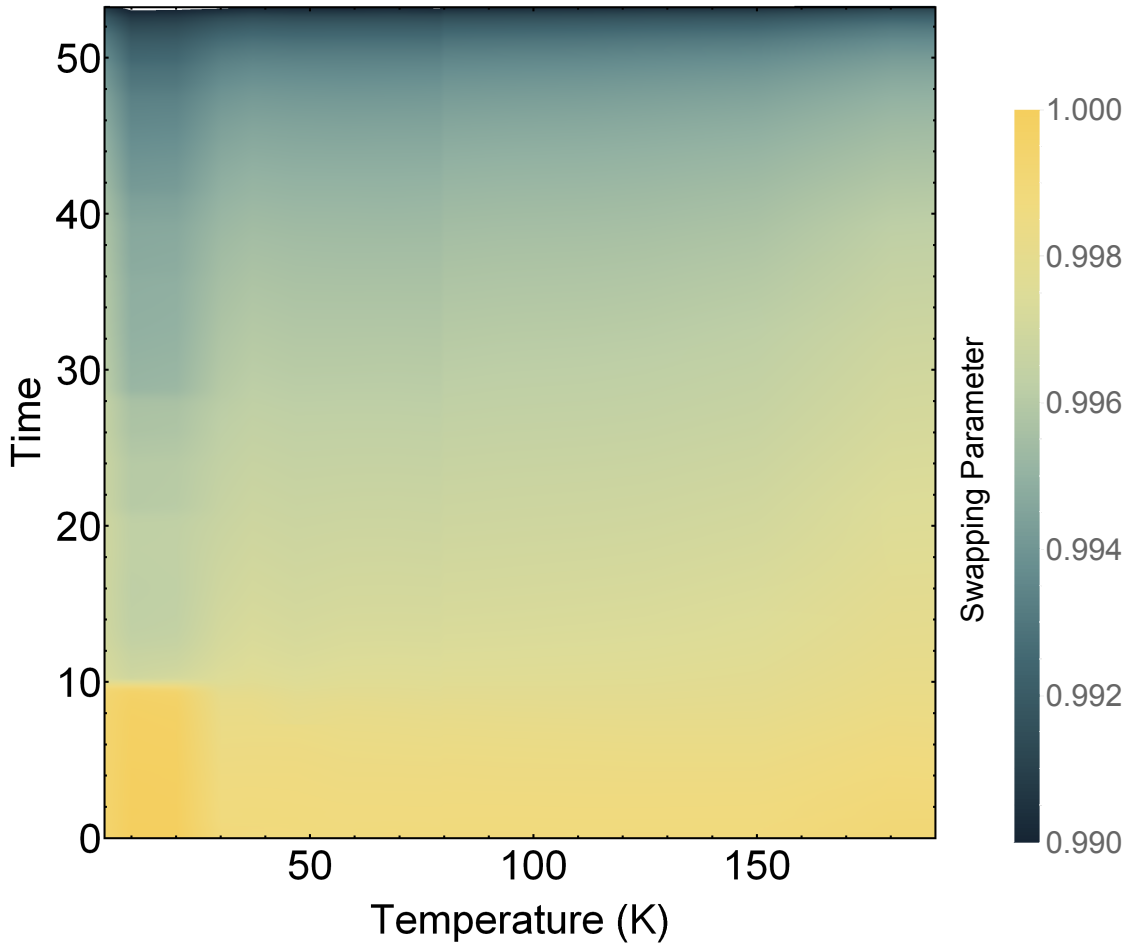


Figure 3.6: Value of the swapping parameter $\langle|\mu|^2\rangle$ against time and temperature. *This parameter controls how much of a partial swap is performed after each interaction with the environment. As can be seen this is very stable for the majority of the time during the experiment, indicating that the model we employ to interpret the data is sound, see Eq. 3.34. The variation towards the end of time period for the experiment is an artifact from the experiment occupying finite time so does not perfectly map to an exponential decay.*

when we build the statistics up from single photon events - we satisfy a thermodynamic relation without having thermodynamic numbers of events to draw upon.

A natural and exciting next step in this program is to prepare two entangled molecules to implement the quantum Maxwell's demon of [59]. This would build on the important first steps we have taken with this work, and reinforce the applicability of

quantum thermodynamics to spectroscopy. A further area of research would be exploring the technological applications of utilizing these organic molecules to probe external fields by employing the relationship between spectroscopy and the Jarzynski equality.

4

Conclusions

Throughout this thesis we have sought to shed some light on two different areas of quantum thermodynamics. We began in Chapter 1 with a brief discussion of classical thermodynamics, and some of the important advancements which have been made in previous years and upon which our own investigations stand. This included the link between thermodynamics and statistical mechanics, the extension of classical thermodynamics from quantities generally concerned with averages to that of single-shot thermodynamics, and finally the fluctuation relations which extend the laws of equilibrium thermodynamics to non-equilibrium regimes.

Having laid this groundwork in Chapter 1, we moved on to a study on the effects of finite time on Landauer's principle of bit reset in Chapter 2. In quasistatic thermodynamics this states that to reset a bit of maximum uncertainty to an exact

value requires the investment of $k_{\mathrm{B}} \ln 2$ of energy. This result is very powerful, and hammers home the important link between the physicality of information and the laws of thermodynamics. However in practical terms, bit reset is never performed in a quasistatic manner – indeed within modern computation we require the investment of many times this level of energy. Despite this, we would like to be able to quantify to what extent carrying out a reset in finite time affects both the quality of a reset and the amount of energy required to perform it. We examined two different protocols – one termed the discrete protocol which consists of alternating periods of energy level shifts and thermalisation, the other continuous protocols in which both of these processes happen simultaneously.

We found that the discrete protocol allows us to perform a bit reset with energy cost close to Landauer's limit – we simply pay an extra cost due to the incomplete thermalisation of the system. Using this protocol we also determined that we could construct a heat engine which operated in finite time at positive power output and efficiency close to the Carnot efficiency. Finally, we constructed a bound on the work fluctuations that showed them to be doubly exponentially suppressed, indicating that the work costs are highly peaked around the average cost. These results were also calculated for the continuous protocol, although unfortunately it does not fare as well in comparison. The extra work cost during the reset is substantially higher than that of the discrete protocol, as we do not have the luxury of thermalising to be closer to the thermal state and instead must invest extra work to overcome the greater occupation of the upper energy level. We also considered the fluctuations present in this protocol and found that for short times they are exponentially expressed whilst for longer time periods they are suppressed by a factor τ^{-1}.

In Chapter 3 we seek to demonstrate that the field of organic molecule fluorescence is particularly well suited to experiments investigating quantum thermodynamical

effects. To this end we first establish a concurrence between the experiment and a theoretical model which satisfies the quantum Jarzynski equality. Having done this we then analyse the experimental data and show that the Jarzynski equality is satisfied at all points throughout the experiment. This suggests to us that the fluorescence of organic molecules is a thermodynamic resource and as such is suitable for continued investigations, such as the implementation of a quantum Maxwell's demon using entangled molecules.

A

Further Details

A.1 Avoiding Quantum Coherences

We can avoid inducing quantum coherences when raising energy levels, by choosing to describe the energy levels by Hamiltonians which are diagonal in the same basis at each stage, written as:

$$\mathcal{H}(n) = \begin{pmatrix} E_1(n) & 0 \\ 0 & E_2(n) \end{pmatrix} = \begin{pmatrix} 0 & 0 \\ 0 & \mathcal{E}n \end{pmatrix}. \tag{A.1}$$

Because they are all diagonal in the same basis, they will always commute; $[\mathcal{H}(n), \mathcal{H}(m)] = 0$ for all n and m. This is a reasonable regime to physically implement, for example, by varying two hyperfine levels in an atom by the application of a time-dependent

external magnetic field.

Defining $P_1(n)$ and $P_2(n)$ as the populations at stage n of lower and upper energy levels respectively, we write the density matrix $\rho(n)$ in the energy eigenbasis as:

$$\rho(n) = \begin{pmatrix} P_1(n) & 0 \\ 0 & P_2(n) \end{pmatrix}. \tag{A.2}$$

In order to apply the Schrödinger equation, we can interpolate into a continuous case and consider the transition from stage n to stage $n+1$ as given by a time parameter t that varies from 0 to τ in each step:

$$\mathcal{H}(n,t) = \begin{pmatrix} 0 & 0 \\ 0 & \mathcal{E}\,(n + t/\tau) \end{pmatrix}, \tag{A.3}$$

such that $\mathcal{H}(n,\tau) = \mathcal{H}(n+1,0)$.

By using the Schrödinger equation to generate an equation for unitary evolution from stage n to stage $n+1$, as we have chosen a $\mathcal{H}$ which commutes with itself throughout the process, we can write down:

$$U(n \to n{+}1) = \exp\left(-\frac{i}{\hbar}\int_0^\tau \mathcal{H}(t)\mathrm{d}t\right). \tag{A.4}$$

$\mathcal{H}(t)$ is always diagonal and so it follows that $\int_0^\tau \mathcal{H}(t)\mathrm{d}t$ must also be diagonal. Taking the exponent of this sum multiplied by a constant $(i/\hbar)$ implies that U must also be a diagonal operator.

The evolution of a state from time $t_i = 0$ (i.e. step n) to time t_f can thus be written as

$$\rho(n{+}1) = U(n \to n{+}1)\ \rho(n)\ U(n \to n{+}1)^\dagger. \tag{A.5}$$

Providing we always start in a diagonal state, all terms on the right hand side are diagonal, and thus $\rho(m)$ is diagonal for all m.

In fact, we can go further and explicitly calculate U due to the simple form of Eq. A.3:

$$\begin{aligned} U(n \to n{+}1) &= \exp\left(-\frac{i}{\hbar}\begin{pmatrix} 0 & 0 \\ 0 & \mathcal{E}\left(n+\frac{1}{2}\right)\tau \end{pmatrix}\right), \\ &= \begin{pmatrix} 1 & 0 \\ 0 & \exp\left(-\frac{i}{\hbar}\mathcal{E}\left(n+\frac{1}{2}\right)\tau\right) \end{pmatrix}. \end{aligned} \tag{A.6}$$

This shows us that the only effect of evolution is to introduce a phase between the upper and lower energy levels, $\phi = \frac{\mathcal{E}}{\hbar}\left(n+\frac{1}{2}\right)\tau$. If the upper and lower energy levels are an incoherent mixture, then this transformation will have no effect whatsoever on the final state; rewriting Eq. A.2 as $\rho(n) = P_1(n)|E_1(n)\rangle\langle E_1(n)| + P_2(n)|E_2(n)\rangle\langle E_2(n)|$, the evolution in Eq. A.5 reduces to

$$\begin{aligned} &\rho(n{+}1) \\ &\quad= U\left(P_1(n)|E_1(n)\rangle\langle E_1(n)| + P_2(n)|E_2(n)\rangle\langle E_2(n)|\right)U^\dagger, \\ &\quad= P_1(n)|E_1(n)\rangle\langle E_1(n)| + P_2(n)e^{-i\phi}|E_2(n)\rangle\langle E_2(n)|e^{i\phi}, \\ &\quad= P_1(n)|E_1(n)\rangle\langle E_1(n)| + P_2(n)|E_2(n)\rangle\langle E_2(n)|, \\ &\quad= \rho(n). \end{aligned} \tag{A.7}$$

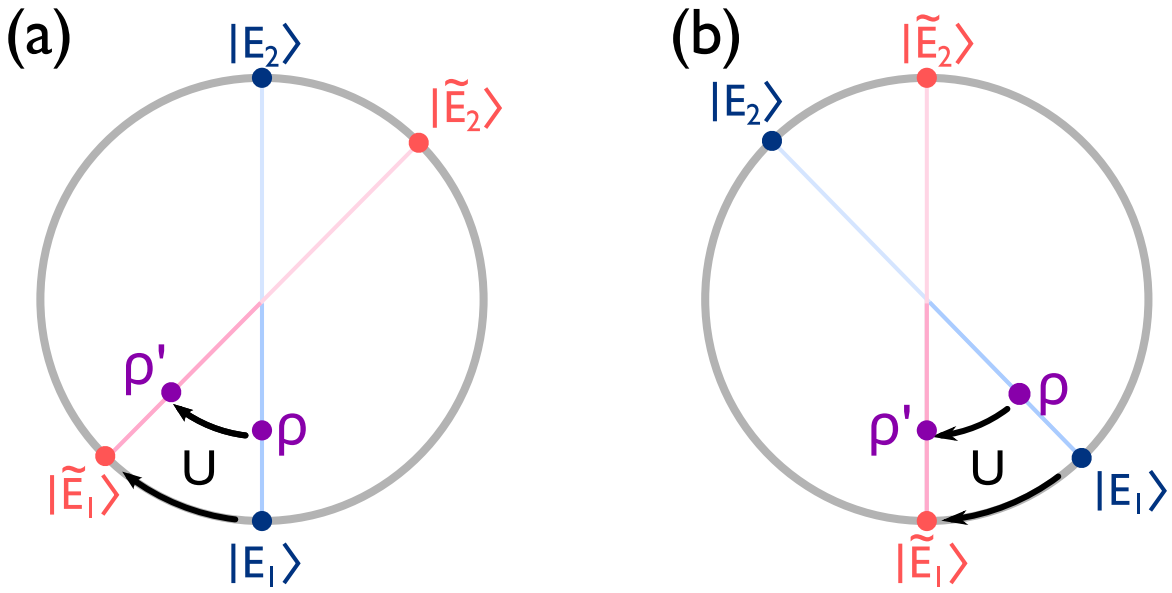


Figure A.1: **Coherent excitation.** *(a) shows the state in the Bloch sphere of the initial Hamiltonian, and (b) of the final. The state ρ, diagonal in the initial Hamiltonian, is a* coherently excited *state in the final Hamiltonian. The same passive transformation U between initial and final Hamiltonians can be applied actively on ρ to map it to ρ', compensating for the work cost of coherent excitation.*

A.2 Active Reversal of the Cost of Coherent Excitations

If the different Hamiltonians are not intrinsically diagonal, we can consider an energy level step as taking us from the initial Hamiltonian $\mathcal{H} = \sum_i E_i |E_i\rangle\langle E_i|$ to the final Hamiltonian $\tilde{\mathcal{H}} = \sum_i \tilde{E}_i |\tilde{E}_i\rangle\langle \tilde{E}_i|$, where not only have the eigenvalues changed, but there is also a change of basis. A change in basis can always be associated with unitary U such that

$$|\tilde{E}_i\rangle\langle\tilde{E}_i| = U|E_i\rangle\langle E_i|U^\dagger, \tag{A.8}$$

and one can express $\tilde{\mathcal{H}} = \sum_i \tilde{E}_i U|E_i\rangle\langle E_i|U^\dagger$.

Consider the initial state of the system, given by a density matrix written diagonally

in the initial Hamiltonian basis: $\rho = \sum_i P_i |E_i\rangle\langle E_i|$. The system energy before the change in Hamiltonian is defined as $\mathrm{Tr}\left(\rho\mathcal{H}\right)$ and afterwards as $\mathrm{Tr}\left(\rho\tilde{\mathcal{H}}\right)$, and so we see that the change in system energy (and thus by conservation of energy, the work cost from reservoir) is given by

$$\Delta W = \mathrm{Tr}(\rho\tilde{\mathcal{H}}) - \mathrm{Tr}(\rho\mathcal{H}). \tag{A.9}$$

To understand why this might result in a work cost, consider the visualisation presented in Figure A.1. We can see that the state ρ appears higher in the sphere in terms of $\tilde{\mathcal{H}}$ than $\mathcal{H}$.

One must take care, however, to note that the energy scale along the vertical axis of each Bloch sphere is different. For bit reset, the energy gap is increasing and $\tilde{E}_2 - \tilde{E}_1 > E_2 - E_1$.

If we were to let the system decohere, the final work cost would be exactly this value (the density matrix in the first term is replaced by a new density matrix with the terms off-diagonal in $\tilde{\mathcal{H}}$ removed; but as these terms only appear inside a trace, they do not contribute to the value).

However, if instead we apply an active unitary transformation on ρ to bring it into a new state ρ', which is diagonal in the new energy eigenbasis $\rho = \sum_i P_i |E_i\rangle\langle E_i| = \sum_i P_i U^\dagger |\tilde{E}_i\rangle\langle\tilde{E}_i| U$ and so the obvious choice is to take $\rho' = U\rho U^\dagger$ given as

$$\rho' = \sum_i P_i |\tilde{E}_i\rangle\langle\tilde{E}_i|. \tag{A.10}$$

If we now consider the overall change in energy between the initial state before the change in Hamiltonian, and the final state after the change in Hamiltonian followed

by the application of the correcting unitary:

$$\begin{aligned}\Delta W &= \mathrm{Tr}(\rho'\tilde{\mathcal{H}}) - \mathrm{Tr}(\rho\mathcal{H}) && \text{(A.11)}\\ &= \mathrm{Tr}\left(\sum_i P_i|\tilde{E}_i\rangle\langle\tilde{E}_i|\sum_j \tilde{E}_j|\tilde{E}_j\rangle\langle\tilde{E}_j|\right) \\ &\quad -\mathrm{Tr}\left(\sum_i P_i|E_i\rangle\langle E_i|\sum_j E_j|E_j\rangle\langle E_j|\right) && \text{(A.12)}\\ &= \sum_i P_i\left(\tilde{E}_i - E_i\right), && \text{(A.13)}\end{aligned}$$

and noting that $\Delta E_i = \tilde{E}_i - E_i$, this recovers the same work cost as if there had been no coherences at all:

$$\Delta W = \sum_i P_i \Delta E_i. \tag{A.14}$$

We have compensated for our passive transformation U on the Hamiltonian basis by actively applying the same transformation to the density matrix. Despite these calculations being demonstrated for the discrete protocol, they are equally valid for the continuous time protocol.

A.3 Bounding the Average Work Cost

In the worst case scenario, at each stage before raising the energy level, we are exactly δ away from the true thermal population. Raising the energy level by $\mathcal{E}$ at stage n has an associated work cost of $P_2(n)\mathcal{E} = \left(P_2^{\mathrm{th}}(n) + \delta\right)\mathcal{E}$. Writing out $P_2^{\mathrm{th}}(n)$ explicitly (using

Eq. 2.3), and summing over all N stages in the bit reset, the (worst case) work cost is

$$\begin{aligned}\langle W\rangle &= \sum_{n=0}^{N}\left(\frac{\exp\left(\frac{-n\mathcal{E}}{k_{\mathrm{B}}T}\right)}{1+\exp\left(\frac{-n\mathcal{E}}{k_{\mathrm{B}}T}\right)}+\right.\\ &+ \left.(1-p)^t\left(\frac{1}{1+\exp\left(\frac{-n\mathcal{E}}{k_{\mathrm{B}}T}\right)}-\frac{1}{2}\right)\right)\mathcal{E}. \end{aligned} \tag{A.15}$$

For small $\mathcal{E}$, we can approximate this sum as an integral and, writing $\mathcal{E}\mathrm{d}n = \mathrm{d}E_2$, and $N\mathcal{E} = E_{\max}$:

$$\begin{aligned}\langle W\rangle &\approx \int_0^{E_{\max}}\mathrm{d}E_2\left(\frac{\exp\left(-\frac{E_2}{k_{\mathrm{B}}T}\right)}{1+\exp\left(-\frac{E_2}{k_{\mathrm{B}}T}\right)}+\right.\\ &\quad \left.+(1-p)^t\left(\frac{1}{1+\exp\left(\frac{-E_2}{k_{\mathrm{B}}T}\right)}-\frac{1}{2}\right)\right)\\ &= \left(1-(1-p)^t\right)k_{\mathrm{B}}T\ln\left(\frac{2}{1+\exp\left(-\frac{E_{\max}}{k_{\mathrm{B}}T}\right)}\right)\\ &\quad +\frac{1}{2}(1-p)^t\left(E_{\max}\right). \end{aligned} \tag{A.16}$$

To interpret this more easily, note that we can define a quantity $\langle W_{\mathrm{quasi}}\rangle$ as the quasistatic work cost of raising the second level to $E_{\max}$:

$$\langle W_{\mathrm{quasi}}\rangle = k_{\mathrm{B}}T\ln\left(\frac{2}{1+\exp\left(-\frac{E_{\max}}{k_{\mathrm{B}}T}\right)}\right). \tag{A.17}$$

The physical relevance of this quantity is simply that it denotes the energy that must be required to perform a bit reset quasistatically, up to a certain point - instead of carrying on raising the second energy level to infinity we stop at some finite

value. Having done this we can see that the average work $\langle W \rangle$ required to raise the upper level from zero to some maximum energy $E_{\max}$, only thermalising for t time steps at each stage, is bounded by

$$\begin{aligned} \langle W_{\text{quasi}} \rangle \;\leq\; \langle W \rangle \;\leq\; & \langle W_{\text{quasi}} \rangle + \\ & (1-p)^t \left(\frac{E_{\max}}{2} - \langle W_{\text{quasi}} \rangle \right). \end{aligned} \tag{A.18}$$

We can see that if $E_{\max} \to \infty$ then $\langle W_{\text{quasi}} \rangle \to k_{\text{B}} T \ln 2$, and we thermalise perfectly ($\delta = 0$), we recover the quasistatic Landauer cost $k_{\text{B}} T \ln 2$ (as derived in Eq. 1). However we can also see that if there is any degree of imperfection in the thermalisation then the work cost of resetting is unboundedly bad due to the non-zero population in the upper energy level throughout the protocol.

A.4 Single-Shot Work Cost

In a single shot classical regime, we assume that at the end of each stage the system is in one of the two energy levels; and we can express each choice of energy level as a sequence of random variables $\{X_i\}_{i=1\ldots N}$. Noting that at each stage, by raising the splitting of the energy levels by $\mathcal{E}$, if the system is in the upper energy state at a particular stage, then this stage contributes a work cost of $\mathcal{E}$. With this in mind, it is useful to label the two energy levels as 0 or 1 such that the work contribution at each stage is given by $X_i \mathcal{E}$, and thus the *actual work cost* of a bit reset is given by the function acting on the random variables:

$$W(X_1, \ldots, X_N) = \mathcal{E} \sum_{i=1}^{N} X_i. \tag{A.19}$$

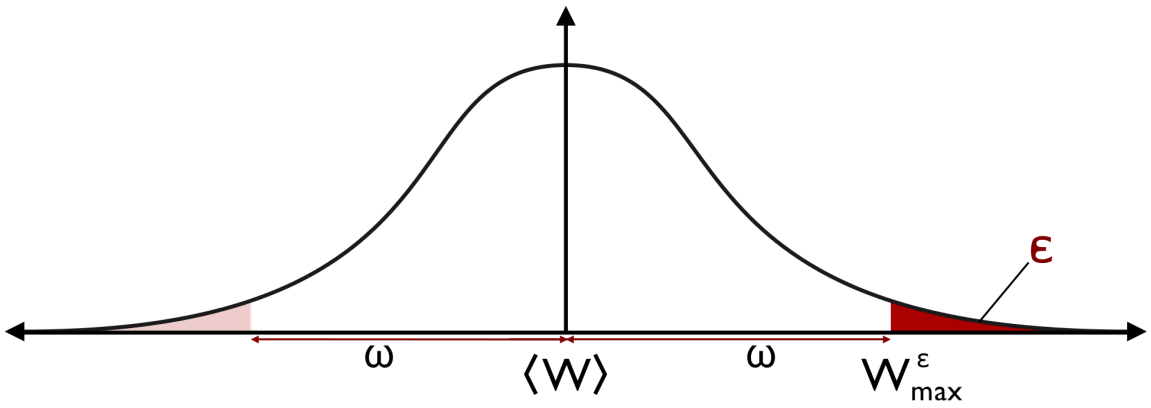


Figure A.2: **An example probabilistic work distribution.** *A repeat of 2.3 for clarity. Work values are always below $W^{\epsilon}_{\max}$, except with probability of failure ϵ given by the area of the shaded region on the right. The sum of the areas of both the shaded regions on the left and right indicates the probability of failing to be within ω of $\langle W \rangle$ (as given by Eq. 2.15).*

It is possible to take the average of this function over some or even all of the random variables. For example, if we take the average over all $X_1 \dots X_N$ we arrive at:

$$\begin{aligned} \langle W(X_1, \dots, X_N) \rangle_{X_1 \dots X_N} & \\ &= \mathcal{E} \sum_{i=1}^{N} \langle X_i \rangle, \\ &= \mathcal{E} \sum_{i=1}^{N} P_2(i) = \langle W \rangle, \end{aligned} \tag{A.20}$$

where $\langle W \rangle$ is the value we would typically call the *average work cost* – the average work cost of the procedure calculated before we know the outcome of any of the random variables. This is the value that we have calculated in the prior sections of this thesis.

There is, in fact, a series of N intermediate stages between W and $\langle W \rangle$, in which given knowledge of the first n values of X_i (that is, the exact cost of the first n steps of the procedure), we make an estimate of what the final work cost will be. This series evolves as a random walk starting at the average value $\langle W \rangle$ and finishing at

the actual value W. Thus if the first n steps of the protocol are in energy levels $X_1 = x_1$, $X_2 = x_2$, etc, then we write the series $D(n)$ as:

$$D(n) = \langle W(x_1, \ldots x_n, X_{n+1}, \ldots, X_N) \rangle_{X_{N-n} \ldots X_N}. \tag{A.21}$$

$D(n)$ undergoes a special type of random walk known as a Doob martingale [84]. It is a martingale because at every step n, the expected value of the next step is the value of the current step:

$$\langle D(n+1) \rangle = D(n). \tag{A.22}$$

For Doob's martingale, this is true by construction as $W(n)$ is defined to be the expectation value of W over future steps.

There is a statistical result known as the Azuma inequality [85] which bounds how far a martingale random walk is likely to deviate from its initial value. When specifically applied to a Doob martingale, this gives us the special case known as the McDiarmid inequality (see 6.10 in [73]) which bounds how far the actual value ($D(N) = W$) deviates from the expectation value ($D(0) = \langle W \rangle$):

$$P(|W - \langle W \rangle| \geq \omega) \quad \leq \quad 2 \exp\left(\frac{-2\,\omega^2}{\sum_{i=1}^{N} |c_n|^2} \right), \tag{A.23}$$

where c_n is the maximum amount our adjustment of the work estimate will change by knowing the outcome of the random variable X_n.

For pedagogical purposes we calculate this expression first for the quasistatic regime of perfect thermalisation (as discussed in the appendices of Egloff and co-authors [13]). In this regime, each X_i is an independent random variable, with a probability distribution given by the thermal populations associated with that

energy level (Eq. 2.3). Switching any particular X_i from 0 to 1 or vice-versa will therefore have at most an effect of $\mathcal{E}$ on W. Hence, $c_i = \mathcal{E}$ for all i, and so we arrive at (repeated here for clarity):

$$P(|W - \langle W \rangle| \geq \omega) \;\leq\; \exp\left(-\frac{2\,\omega^2}{N\mathcal{E}^2}\right). \tag{A.24}$$

When we enter the finite time regime, in which thermalisation is only partially achieved, X_i are no longer perfectly independent. If we treat P_{swap} as the probability over the entire period of thermalisation that we exchange our system with the thermal state, then X_{i+1} will take the value of X_i with probability $(1 - P_{\text{swap}})$, and only with probability P_{swap} will it be given by the random thermal distribution.

To calculate the impact of exchanging one stage X_n, we must explicitly evaluate the difference between $D(n) = \langle W(x_1, \ldots x_{n-1}, 0, X_{n+1}, \ldots, X_N)\rangle_{X_{N-n}\ldots X_N}$ and $\langle W(x_1, \ldots x_{n-1}, 1, X_{n+1}, \ldots, X_N)\rangle_{X_{N-n}\ldots X_N}$. To evaluate this, it is necessary to consider the expectation work cost at every stage of the protocol between n and the end (N), and how this changes depending on the value of X_n.

We recall the stochastic matrix for evolution between a state n and $n+1$ can be written as $M(n)$, given in Eq. 2.4. The stochastic evolution from state n to $n+k$ is thus given by the left-product of matrices

$$\mathcal{M}(n \to n+k) = M(n+k-1)\ldots M(n+1)M(n). \tag{A.25}$$

The form of $M_{\text{swap}}(n)$ allows us to simplify this product. Over k steps are there are $k+1$ possible outcome states of the system corresponding swapping with one of the thermal states $\mathbf{P}^{\text{th}}(n+j)$ (where $j = 0 \ldots k-1$) or doing nothing at all. Because of the nature of a swap operation (in particular because P_{swap} is independent of the state of the

system), only the final swap is important – all intermediate swaps will be 'overwritten'. This means there is always a probability of P_{swap} that the system is in the state it last had some chance of swapping with (i.e. $\mathbf{P}^{\text{th}}(n+k-1)$). Provided it has not swapped with this state, there is then a chance P_{swap} that the system has swapped into the state before it – giving an overall probability of swapping into this state of $(1-P_{\text{swap}})P_{\text{swap}}$. Working backwards with this logic, we see that the probability of the system after k steps being in the state associated with swapping after j steps is $(1-P_{\text{swap}})^{k-j}P_{\text{swap}}$. Finally, we note that the only way for the system to have not changed at all is for it to have not swapped at any of the opportunities; and this has a probability of $(1-P_{\text{swap}})^k$. With all of this in mind, we can now write out $\mathcal{M}(n \to n+k)$ in a simple linear form:

$$\begin{aligned}\mathcal{M}(n \to n+k) &= (1-P_{\text{sw}})^k \mathbb{1} \\ &\quad + P_{\text{sw}} \sum_{j=0}^{k-1} (1-P_{\text{sw}})^{k-j-1} M_{\text{th}}(n+j),\end{aligned} \tag{A.26}$$

where $M_{\text{th}}(i)$ (as defined in Eq. 2.5) is the matrix that perfectly exchanges any state with the thermal state $\mathbf{P}^{\text{th}}(i)$. If $P_{\text{swap}} = 1$, then $\mathcal{M}$ reduces to the thermalising matrix for the final stage $M_{\text{th}}(n+k-1)$.

The expected energy cost of step $n+k$ given that the state starts in the lower energy level is then given by the top right component of $\mathcal{M}$ multiplied by $\mathcal{E}$, and the expected cost if the state starts in the upper energy level is given by the lower right component multiplied by $\mathcal{E}$. We can thus express the difference between these two values as

$$\mathcal{E} \begin{pmatrix} 0 & 1 \end{pmatrix} \mathcal{M}(n \to n+k) \begin{pmatrix} 1 \\ -1 \end{pmatrix}. \tag{A.27}$$

Again, considering the special case $P_{\text{swap}} = 1$, we note that this value is zero for all $k \geq 1$; the change in expected contribution from all future steps as a result of altering

the current state is zero when the future steps are independent of the current state.

Finally, we write out the predicted difference in estimated final work cost, c_n, as the sum:

$$c_n = \begin{pmatrix} 0 & \mathcal{E} \end{pmatrix} \left(\mathbb{1} + \sum_{k=1}^{N} \mathcal{M}(n \to n+k) \right) \begin{pmatrix} 1 \\ -1 \end{pmatrix}. \tag{A.28}$$

In this most general form, the expression is difficult to evaluate analytically. However, noting that the components of M_{th} are the thermal populations at each stage, which are in the range $[0, 1]$, we can bound the sum:

$$0 \leq \sum_j (1 - P_{\text{sw}})^j P^{\text{th}}(j) \leq \sum_j (1 - P_{\text{sw}})^j \begin{pmatrix} 1 & 1 \\ 1 & 1 \end{pmatrix}. \tag{A.29}$$

Evaluating equation A.28 effectively involves subtracting the bottom right element of the matrix in the middle from the bottom left. And as a maximal value of $|c_n|$ would be the most deleterious for our bound (causing the widest spread of work values from the mean) we therefore take the upper bound on this sum for the bottom right and the lower bound for the bottom left.

This allows us to bound $|c_n|$ by:

$$|c_n| \leq \mathcal{E} \frac{1 - (1 - P_{\text{sw}})^{N-n}}{P_{\text{sw}}}. \tag{A.30}$$

This tells us that when we are far away from the end of the protocol, such that $n \ll N$, the effect of changing one stage has an effect that scales like $1/P_{\text{sw}}$. Closer to the end of the protocol, the effect is diminished, as there are fewer chances to swap, which thus truncates the influence.

We consider the sum of terms $\sum_n |c_n|^2$, as required for the McDiarmid inequality

(Eq. A.23):

$$\sum_n |c_n|^2 \leq \frac{\mathcal{E}^2}{P_{\rm sw}^2} \sum_n \left(1 - (1 - P_{\rm sw})^{N-n}\right)^2. \tag{A.31}$$

The leading term of the sum is N, and so again we can upper bound this value:

$$\sum_n |c_n|^2 \leq \frac{N\mathcal{E}^2}{P_{\rm sw}^2}. \tag{A.32}$$

By taking only the first term we slightly over-estimate the importance of a change at one step. This approximation encodes the assumption that any change has the full number of chances to influence the state. This means the bound we place on the deviation away from the average value of work is not as tight as it might otherwise be. We finally substitute this value into the McDiarmid inequality to arrive at the probability of differing from the average work cost by a certain amount:

$$P(|W - \langle W \rangle| \geq \omega) \;\; \leq \;\; \exp\left(-\frac{2\,\omega^2 {P_{\rm sw}}^2}{N\mathcal{E}^2}\right). \tag{A.33}$$

A.5 Calculating $W_{\rm max}^{\epsilon}$.

We can express the above result in the language of single-shot statistics by calculating the maximum work, except with some probability of failure ϵ, defined:

$$P(W > W_{\rm max}^{\epsilon}) := \epsilon, \tag{A.34}$$

or equivalently $W_{\rm max}^{\epsilon}$ is defined by the integral

$$\int_{-\infty}^{W_{\rm max}^{\epsilon}} P(W) \mathrm{d}W = 1 - \epsilon. \tag{A.35}$$

We can re-centre this definition around the expectation value of work, $\langle W \rangle$, such that:

$$P\Big(W - \langle W \rangle > W^{\epsilon}_{\max} - \langle W \rangle\Big) = \epsilon, \tag{A.36}$$

and in this form, we note that ϵ can be bounded by Eq. 8, with $\omega = W^{\epsilon}_{\max} - \langle W \rangle$ (see Figure 2.3):

$$\epsilon \leq \ 2\exp\left(-\frac{2\,\left(W^{\epsilon}_{\max} - \langle W \rangle\right)^2 {P_{\rm sw}}^2}{N\mathcal{E}^2}\right). \tag{A.37}$$

Re-arranging, we arrive at an upper bound on $W^{\epsilon}_{\max}$:

$$W^{\epsilon}_{\max} \leq \langle W \rangle + \frac{\mathcal{E}}{P_{\rm sw}}\sqrt{\frac{N\ln(2/\epsilon)}{2}}, \tag{A.38}$$

or explicitly in terms of thermalising time:

$$W^{\epsilon}_{\max} \leq \langle W \rangle + \frac{\mathcal{E}}{1-(1-p)^t}\sqrt{\frac{N\ln(2/\epsilon)}{2}}. \tag{A.39}$$

We combine this bound with the influence of finite time on $\langle W \rangle$ to get:

$$\begin{aligned} W^{\epsilon}_{\max} \ &\leq \ \langle W_{\rm quasi} \rangle + \frac{1}{2}(1-p)^t N\mathcal{E} \\ &+ \ \frac{1}{1-(1-p)^t}\sqrt{\frac{\ln(2/\epsilon)}{2N}}N\mathcal{E}. \end{aligned} \tag{A.40}$$

A.6 A Continuous Time Protocol

It may be wondered how many of these results are dependent upon the discrete time protocol where we perform each aspect of the reset separately. To this end let us examine a continuous time version of the same protocol. As a starting of point, the original

protocol consists of two ingredients – we perform discrete changes to the Hamiltonian:

$$\begin{aligned} E_1(0) &= E_1(t) = 0, \\ E_2(t) &= t\varepsilon, \end{aligned} \tag{A.41}$$

and we thermalise via partial swap for some number of steps t:

$$\begin{aligned} \tilde{S} &= (1-q)\mathbb{1} + q|\text{unit}\rangle\langle T(t)|, \\ &= \frac{1}{Z_t}\begin{pmatrix} Z_t(1-q)+q & q \\ q\mathrm{e}^{-t\beta\varepsilon} & Z_t(1-q)+q\mathrm{e}^{-t\beta\varepsilon} \end{pmatrix} \end{aligned} \tag{A.42}$$

To take this to the continuous time we change the Hamiltonian linearly according to:

$$\begin{aligned} E_1(t) &= 0, \\ E_2(t) &= \frac{t}{\tau}E_{\max}, \end{aligned} \tag{A.43}$$

where $E_{\max} \equiv N\varepsilon$ and τ is the time period over which the energy is changed. We also need to determine the infinitesimal version of thermalisation under the partial swap model. To this end, consider an infinitesimal timestep δt and let the probability of not performing a swap be $\alpha^{\delta t}$ so that thermalisation is slow. Then we have:

$$\begin{aligned} P(\neg\text{swap}) &= \alpha^{\delta t}, \\ P(\text{swap}) &= 1-\alpha^{\delta t}. \end{aligned} \tag{A.44}$$

Since we desire $P(\text{swap}) \approx O^+$ we let $\alpha = (1-\gamma)$ and expand for short times:

$$\begin{aligned} P(\text{swap}) &= 1-(1-\gamma)^{\delta t} \\ &= 1-1+\gamma\delta t+\mathcal{O}(\delta t^2) \\ &\approx \gamma\delta t. \end{aligned} \tag{A.45}$$

Now we write $\tilde{S}$ for an infinitesimal time step:

$$\begin{aligned} \tilde{S} &= \begin{pmatrix} 1-\gamma\delta t(1-\frac{1}{Z(t)}) & \gamma\delta t\frac{1}{Z(t)} \\ \gamma\delta t\frac{\mathrm{e}^{-\beta E^1(t)}}{Z(t)} & 1-\gamma\delta t\left(1-\frac{\mathrm{e}^{-\beta E^1(t)}}{Z(t)}\right) \end{pmatrix} \\ &= \mathbb{1}-\gamma\delta t\begin{pmatrix} 1-\frac{1}{Z(t)} & -\frac{1}{Z(t)} \\ -\frac{\mathrm{e}^{-\beta E^1(t)}}{Z(t)} & 1-\frac{\mathrm{e}^{-\beta E^1(t)}}{Z(t)} \end{pmatrix} \\ &\equiv \mathbb{1}-\gamma\delta t\tilde{Q}. \end{aligned} \tag{A.46}$$

A.7 Bounding the Average Work for a Continuous Protocol

We are now in a position to consider the infinitesimal evolution of the probability distribution and hence derive the differential equations controlling their subsequent evolutions:

$$\begin{aligned} \mathbf{p}+\delta\mathbf{p} &= \tilde{S}\mathbf{p} \\ &= \left(\mathbb{1}-\gamma\delta t\tilde{Q}\right)\mathbf{p} \\ \Rightarrow \delta\mathbf{p} &= -\gamma\delta t\tilde{Q}\mathbf{p}, \\ \Rightarrow \frac{\mathrm{d}\mathbf{p}}{\mathrm{d}t} &= -\gamma\tilde{Q}\mathbf{p}. \end{aligned} \tag{A.47}$$

This equation then makes it obvious what γ is – namely the rate at which we thermalise the system by interacting with the bath. Writing this out explicity we find that:

$$\frac{\mathrm{d}}{\mathrm{d}t}\begin{pmatrix} p_1 \\ p_2 \end{pmatrix} = -\gamma \begin{pmatrix} p_1 - \frac{1}{Z(t)} \\ p_2 - \frac{\mathrm{e}^{-\frac{\beta E_{\max}}{\tau}t}}{Z(t)} \end{pmatrix}. \tag{A.48}$$

Despite their simple form these equations do not have simple solutions. By using Mathematica we find that they admit hypergeometric functions as their solutions, reproduced here for completeness:

$$\begin{aligned} p_2(t) = \frac{1}{2}\mathrm{e}^{-\gamma t} \quad &+ \quad \frac{\kappa}{2}\,\psi\left(\frac{\kappa}{2}\right) - \frac{\kappa}{2}\psi\left(\frac{1}{2}\left(1+\kappa\right)\right) \\ &+ \quad {}_2F_1\left(1,\kappa;1+\kappa;-\mathrm{e}^{-\frac{\kappa}{\gamma}t}\right) \end{aligned} \tag{A.49}$$

where $\kappa = \gamma\tau/\beta E_{\max}$, $\psi(z)$ is the polygamma function (see [71]) and ${}_2F_1(a,b;c;z)$ is the hypergeometric function (see [72]). These functions are not easy to use in further calculations to determine things like the average work cost, nor do they lend themselves well to developing an intuitive sense of what the mathematics represents in terms of the system behaviour.

Since $p_1 + p_2 = 1$ we focus on the evolution of p_2 as it contributes to the cost of performing a reset, and we proceed by bounding the evolution of the probability distribution using the fact that $1 \leq Z(t) \leq 2$ so that we have:

$$-\gamma\left(p_2 - \frac{1}{2}\mathrm{e}^{\frac{\beta E_{\max}}{\tau}t}\right) \leq p_2(t) \leq -\gamma\left(p_2 - \mathrm{e}^{\frac{\beta E_{\max}}{\tau}t}\right) \tag{A.50}$$

Solving this we find:

$$\begin{aligned} p_2^{\text{lower}}(t) &\geq \frac{\kappa+1}{2(\kappa-1)}\mathrm{e}^{-\gamma t} - \frac{\kappa}{2(\kappa-1)}\mathrm{e}^{-\frac{\gamma}{\kappa}t}, \\ p_2^{\text{upper}}(t) &\leq \frac{2\kappa+1}{2(\kappa-1)}\mathrm{e}^{-\gamma t} - \frac{\kappa}{(\kappa-1)}\mathrm{e}^{-\frac{\gamma}{\kappa}t}, \end{aligned} \tag{A.51}$$

where we have written $\kappa = \gamma\tau/\beta E_{\text{max}}$ as before for ease of notation. We can now calculate bounds on the average work cost for performing a reset. As in the discrete time process, the average work cost is given by:

$$\langle W \rangle = \int_0^{E_{\text{max}}} p_2(t)\mathrm{d}E_1 = -\frac{\gamma}{\kappa}\int_0^{\tau} p_2(t)\mathrm{d}t \tag{A.52}$$

To aid legibility we split the upper and lower bounds to the average work:

$$\begin{aligned} \langle W_{\text{lower}} \rangle &\geq -\frac{\gamma}{\kappa}\int_0^{\tau} p_2^{lower}(t)\mathrm{d}t \\ &\geq \frac{\kappa+1}{2\kappa(\kappa-1)}\left(\mathrm{e}^{-\gamma\tau}-1\right) + \frac{\kappa}{2(\kappa-1)}\left(1-\mathrm{e}^{-\beta E_{\text{max}}}\right) \\ &\geq \frac{\gamma\tau+\beta E_{\text{max}}}{\gamma\tau-\beta E_{\text{max}}}\frac{\beta E_{\text{max}}}{2\gamma\tau}\left(\mathrm{e}^{-\gamma\tau}-1\right) + \frac{\gamma\tau}{2\left(\gamma\tau-\beta E_{\text{max}}\right)}\left(1-\mathrm{e}^{-\beta E_{\text{max}}}\right) \end{aligned} \tag{A.53}$$

$$\begin{aligned} \langle W_{\text{upper}} \rangle &\leq -\frac{\gamma}{\kappa}\int_0^{\tau} p_2^{upper}(t)\mathrm{d}t \\ &\leq \frac{2\kappa+1}{2\kappa(\kappa-1)}\left(\mathrm{e}^{-\gamma\tau}-1\right) + \frac{\kappa}{(\kappa-1)}\left(1-\mathrm{e}^{-\beta E_{\text{max}}}\right) \\ &\leq \frac{2\gamma\tau+\beta E_{\text{max}}}{\gamma\tau-\beta E_{\text{max}}}\frac{\beta E_{\text{max}}}{2\gamma\tau}\left(\mathrm{e}^{-\gamma\tau}-1\right) + \frac{\gamma\tau}{\gamma\tau-\beta E_{\text{max}}}\left(1-\mathrm{e}^{-\beta E_{\text{max}}}\right) \end{aligned} \tag{A.54}$$

Bibliography

[1] A. S. Eddington. The nature of the physical world. *Cambridge University Press*, 1928.

[2] R. Landauer. The physical nature of information. *Physics Letters A*, 217:188–193, 1996.

[3] C. J. Adkins. Equilibrium thermodynamics. *Cambridge University Press*, 1983.

[4] H. B. Callen. Thermodynamics and an introduction to thermostatistics. *Wiley*, 1985.

[5] J. Gemmer, M. Michel, and G. Mahler. Quantum thermodynamics: Emergence of thermodynamic behavior within composite quantum systems. *Springer Berlin Heidelberg*, 2009.

[6] S. Blundell and K.M. Blundell. Concepts in thermal physics. *OUP Oxford*, 2010.

[7] D. Kondepudi and I. Prigogine. Modern thermodynamics: From heat engines to dissipative structures. *Wiley*, 2014.

[8] G. Mahler. Quantum thermodynamic processes: Energy and information flow at the nanoscale. *Pan Stanford Publishing*, 2014.

[9] C. Jarzynski. Nonequilibrium equality for free energy differences. *Phys. Rev. Lett.*, 78:2690–2693, Apr 1997.

[10] G. E. Crooks. The entropy production fluctuation theorem and the nonqueilibrium work relation for free energy differences. *Physical Review E*, 60(3):2721–2726, September 1999. arXiv:cond-mat/9901352.

[11] H. Tasaki. Jarzynski relations for quantum systems and some applications. *arXiv:cond-mat/0009244*, September 2000.

[12] J. Goold, M. Huber, A. Riera, L. del Rio, and P. Skrzypzyk. The role of quantum information in thermodynamics — a topical review. *Journal of Physics A*, February 2016.

[13] S. Vinjanampathy and J. Anders. Quantum thermodynamics. *Contemporary Physics*, 57(4):545–579, 2016.

[14] J. Aberg. Truly work-like work extraction. *Nature Communications*, 4(1925), 2011/2013. arXiv:1110.6121.

[15] O. C. O. Dahlsten, R. Renner, E. Rieper, and V. Vedral. Inadequacy of von Neumann entropy for characterizing extractable work. *New Journal of Physics*, 13(5):053015, 2011.

[16] D. Egloff, O. C. O. Dahlsten, R. Renner, and V. Vedral. Laws of thermodynamics beyond the von Neumann regime. *arXiv:quant-ph/1207.0434*, July 2012.

[17] D. Janzing, P. Wocjan, R. Zeier, R. Geiss, and T. Beth. The thermodynamic cost of reliability and low temperatures: Tightening landauer's principle and the second law. *International Journal of Theoretical Physics*, 39:2217 – 2753, 2000.

[18] M. Horodecki and J. Oppenheim. Fundamental limitations for quantum and nano thermodynamics. *Nature Communications*, 4(2059), 2011/2013. arXiv:1111.3834.

[19] F. Brandão, M. Horodecki, N. Ng, J. Oppenheim, and S. Wehner. The second laws of quantum thermodynamics. *Proceedings of the National Academy of Sciences*, 112(11):3275–3279, 2015.

[20] M. Lostaglio, D. Jennings, and T. Rudolph. Thermodynamic resource theories, non-commutativity and maximum entropy principles. *New Journal of Physics*, 19, 2017.

[21] J. Liphardt, S. Dumont, S. B. Smith, I. Tinoco, and C. Bustamante. Equilibrium information from nonequilibrium measurements in an experimental test of jarzynski's equality. *Science*, 296(5574):1832–1835, 2002.

[22] F. Douarche, S. Ciliberto, A. Petrosyan, and I. Rabbiosi. An experimental test of the jarzynski equality in a mechanical experiment. *EPL (Europhysics Letters)*, 70(5):593, 2005.

[23] T. Batalhão, A. M. Souza, L. Mazzola, R. Auccaise, I. S. Oliveira, J. Goold, G. De Chiara, M. Paternostro, and R. M. Serra. Experimental reconstruction of work distribution and verification of fluctuation relations at the full quantum level. *Physical Review Letters*, 113(14), October 2014. arXiv:1308.3241.

[24] S. An, J. N. Zhang, M. Um, D. Lv, Y. Lu, J. Zhang, Z. Q. Yin, H. T. Quan, , and K. Kim. Experimental test of the quantum Jarzynski equality with a trapped-ion system. *Nature Physics*, 11(2):193 – 199, February 2015.

[25] R. Klages, W. Just, and C. Jarzynski. Nonequilibrium statistical physics of small systems: Fluctuation relations and beyond. *Wiley*, 2013.

[26] M. Campisi, P. Hänggi, and P. Talkner. Quantum fluctuation relations: Foundations and applications. *Rev. Mod. Phys.*, 83:771–791, Jul 2011.

[27] M. Borrelli, J. V. Koski, S. Maniscalco, and J. P. Pekola. Fluctuation relations for driven coupled classical two-level systems with incomplete measurements. *Phys. Rev. E*, 91:012145, Jan 2015.

[28] M. Mehboudi, A. Sanpera, and J. M. R. Parrondo. Generalized fluctuation-dissipation relation for quantum markovian systems. *arXiv:1705.03968*, 2017.

[29] D. Chandler. Introduction to modern statistical mechanics. *Oxford University Press*, 1987.

[30] Oscar C. O. Dahlsten. Non-equilibrium statistical mechanics inspired by modern information theory. *Entropy*, 15(12):5346–5361, 2013.

[31] R. Renner. Security of quantum key distribution. *arXiv*, 2005. arXiv:quant-ph/0512258.

[32] R. Alicki, M. Horodecki, P. Horodecki, and R. Horodecki. Thermodynamics of quantum information systems Hamiltonian description. *Open Systems & Information Dynamics*, 11(3):205–217, 2004.

[33] J. C. Maxwell. Theory of Heat. *Longmans, Green & Co*, pages 338–339, 1870.

[34] L. Szilard. über die Enfropieuerminderung in einem thermodynamischen System bei Eingrifen intelligenter Wesen. *Zeitschrift für Physik*, 53:840–856, 1929.

[35] H. Leff and A. F. Rex. Maxwell's Demon 2: Entropy, Classical and Quantum Information, Computing. *Taylor & Francis*, 2002.

[36] L. Brillouin. Maxwell's demon cannot operate: Information and entropy i. *Journal of Applied Physics*, 22:334, 1951.

[37] L. Brillouin. Physical entropy and information ii. *Journal of Applied Physics*, 22:338, 1951.

[38] R. Landauer. Irreversibility and heat generation in the computing process. *IBM Journal of Research and Development*, 5:183 – 191, jul 1961.

[39] A. C. Barato and U. Seifert. An autonomous and reversible maxwell's demon. *EPL (Europhysics Letters)*, 101(6):60001, 2013.

[40] A. Chapman and A. Miyake. How an autonomous quantum maxwell demon can harness correlated information. *Phys. Rev. E*, 92:062125, Dec 2015.

[41] J. V. Koski, A. Kutnoven, I. M. Khaymovich, T. Ala-Nissila, and J. P. Pekola. On-Chip Maxwell's Demon as an Information-Powered Refrigerator. *Physical Review Letters*, 115(26), December 2015.

[42] A. Kutnoven, J. V. Koski, and T. Ala-Nissila. Thermodynamics and efficiency of an autonomous on-chip maxwell's demon. *Scientific Reports*, 6, February 2016.

[43] N. G. Anderson. Conditioning, correlation and entropy generation in maxwell's demon. *Entropy*, 15(10):4243 – 4265, 2013.

[44] T. Sagawa and M. Ueda. Information thermodynamics: Maxwell's demon in nonequilibrium dynamics. *Wiley-VCH Verlag GmbH & Co. KGaA*, pages 181–211, 2013.

[45] J. V. Koski, V. F. Maisi, T. Sagawa, and J. P. Pekola. Experimental observation of the role of mutual information in the nonequilibrium dynamics of a maxwell demon. *Phys. Rev. Lett.*, 113:030601, Jul 2014.

[46] N. Shiraishi, S. Ito, K. Kawaguchi, and T. Sagawa. Role of measurement-feedback separation in autonomous maxwell's demons. *New Journal of Physics*, 17(4):045012, 2015.

[47] S. Lloyd. Quantum-mechanical maxwell's demon. *Phys. Rev. A*, 56:3374–3382, Nov 1997.

[48] W. H. Zurek. Maxwell's Demon, Szilard's Engine and Quantum Measurements. *arXiv*, January 2003.

[49] S. W. Kim, T. Sagawa, S. De Liberato, and M. Ueda. Quantum szilard engine. *Phys. Rev. Lett.*, 106:070401, Feb 2011.

[50] J. J. Park, K. Kim, T. Sagawa, and S. W. Kim. Heat engine driven by purely quantum information. *Phys. Rev. Lett.*, 111:230402, Dec 2013.

[51] P. A. Camati, J. P. S. Peterson, T. B. Batalhão, K. Micadei, A. M. Souza, R. S. Sarthour, I. S. Oliveira, and R. M. Serra. Experimental rectification of entropy production by maxwell's demon in a quantum system. *Phys. Rev. Lett.*, 117:240502, Dec 2016.

[52] J. Thorn, E. Schoene, T. Li, and D. Steck. Experimental Realization of an Optical One-Way Barrier for Neutral Atoms. *Physical Review Letters*, 100(24), June 2008.

[53] S. Toyabe, T. Sagawa, M. Ueda, E. Muneyuki, and M. Sano. Experimental demonstration of information-to-energy conversion and validation of the generalized Jarzynski equality. *Nature Physics*, 6(12):988–992, November 2010.

[54] E. Aurell, C. Mejia-Monasterio, and P. Muratore-Ginanneschi. Optimal protocols and optimal transport in stochastic thermodynamics. *Physical Review Letters*, 106(25), June 2011. arXiv: 1012.2037.

[55] J. V. Koski, V. F. Maisi, J. P. Pekola, and D. V. Avering. Experimental realization of a Szilard engine with a single electron. *Proceedings of the National Academy of Sciences of the United States of America*, 111(38):13786 – 13789, August 2014.

[56] C. Browne, A. J. P. Garner, O. C. O. Dahlsten, and V. Vedral. Guaranteed energy-efficient bit reset in finite time. *Phys. Rev. Lett.*, 113:100603, Sep 2014.

[57] C. H. Bennett. The thermodynamics of computation—a review. *International Journal of Theoretical Physics*, 21(12):905–940, December 1982.

[58] M. P. Frank. Approaching the physical limits of computing. *2013 IEEE 43rd International Symposium on Multiple-Valued Logic*, 0:168–185, 2005.

[59] L. del Rio, J. Aberg, R. Renner, O. C. O. Dahlsten, and V. Vedral. The thermodynamic meaning of negative entropy. *Nature*, 474(7349):61–3, June 2011.

[60] A. Bérut, A. Arakelyan, A. Petrosyan, S. Ciliberto, R. Dillenschneider, and E. Lutz. Experimental verification of Landauer's principle linking information and thermodynamics. *Nature*, 483(7388):187–9, March 2012.

[61] K. Sekimoto and S. Sasa. Complementarity relation for irreversible process derived from stochastic energetics. *Journal of the Physical Society of Japan*, 66(11):3326–3328, November 1997.

[62] V. Serreli, C. Lee, E. R. Kay, and D. A. Leigh. A molecular information ratchet. *Nature*, 445(7127):523–7, February 2007.

[63] J. Bergli, Y. M. Galperin, and N. B. Kopnin. Information flow and optimal protocol for maxwell's demon single electron pump. *Physical Review E*, 88(6), December 2013. arXiv: 1306.2742.

[64] P. R. Zulkowski and M. R. DeWeese. Optimal finite-time erasure of a classical bit. *arXiv:1310.4167 [cond-mat]*, October 2013.

[65] T. D. Kieu. The Second Law, Maxwell's Demon, and Work Derivable from Quantum Heat Engines. *Phys. Rev. Lett.*, 93(14), September 2004.

[66] H. T Quan. and H. Dong. Quantum crooks fluctuation theorem and quantum jarzynski equality in the presence of a reservoir. *arXiv:quant-ph/0812.4955*, December 2008. arXiv: 0812.4955.

[67] M. V. Berry. Transitionless quantum driving. *Journal of Physics A: Mathematical and Theoretical*, 42(36):365303, September 2009.

[68] S. Deffner, C. Jarzynski, and A. del Campo. Classical and quantum shortcuts to adiabaticity for scale-invariant driving. *Physical Review X*, 4(2), April 2014. arXiv: 1401.1184.

[69] A. del Campo, J. Goold, and M. Paternostro. More bang for your buck: Towards super-adiabatic quantum engines. *arXiv:1305.3223 [cond-mat, physics:quant-ph]*, May 2013. arXiv: 1305.3223.

[70] D. A. Levin, Y. Peres, and E. L. Wilmer. Markov chains and mixing times. *American Mathematical Soc.*, page 371, 2009.

[71] M. Abramowitz and I. A. Stegun. Handbook of mathematical functions. *Dover Publications*, 1964.

[72] K. F. Riley, M. P. Hobson, and S. J. Bence. Mathmatical methods for physics and engineering. *Cambridge University Press*, pages 628 – 630, 2006.

[73] C. McDiarmid. On the method of bounded differences. *London Mathematical Society Lecture Note Series*, 141, 1989.

[74] M. Mitzenmacher and E. Upfal. Probability and computing. *Cambridge University Press*, 2005.

[75] P. Faist, F. Dupuis, J. Oppenheim, and R. Renner. A Quantitative Landauer's Principle. *ArXiv e-prints*, November 2012. arXiv:1211.1037.

[76] C. Browne, T. Farrow, O. C. O. Dahlsten, and V. Vedral. Organic molecule fluorescence as an experimental test-bed for quantum jumps in thermodynamics. *Proceedings of the Royal Society of London A: Mathematical, Physical and Engineering Sciences*, 473(2204), 2017.

[77] F. W. J. Hekking and J. P. Pekola. Quantum jump approach for work and dissipation in a two-level system. *Physical Review Letters*, 111(9), August 2013. arXiv: 1305.5207.

[78] R. F. Fox. Using nonequilibrium measurements to determine macromolecule free-energy differences. *Proceedings of the National Academy of Sciences of the United States of America*, 100(22):12537–12538, October 2003. arXiv:cond-mat/9901352.

[79] S. Park, F. Khalili-Araghi, E. Tajkhorshid, and K. Schulten. Free energy calculation from steered molecular dynamics simulations using Jarzynski's equality. *The Journal of Chemical Physics*, 119(6):3559–3566, August 2003.

[80] F. M. Ytreberg and D. M. Zuckerman. Efficient use of nonequilibrium measurement to estimate free energy differences for molecular systems. *Journal of Computational Chemistry*, 25(14):1749–1759, November 2004.

[81] C. Jarzynski and D. K. Wójcik. Classical and Quantum Fluctuation Theorems for Heat Exchange. *Physical Review Letters*, 292(23), June 2004.

[82] W. E. Moerner. Nobel lecture: Single-molecule spectroscopy, imaging, and photocontrol: Foundations for super-resolution microscopy. *Rev. Mod. Phys*, 87(1183), 2015.

[83] M. B. Plenio and P. L. Knight. The Quantum Jump Approach to Dissipative Dynamics in Quantum Optics. *Reviews of Modern Physics*, 70(1):101 – 144, January 1998. arXiv:quant-ph/9702007.

[84] J. L. Doob. Regularity properties of certain families of chance variables. *Transactions of the American Mathematical Society*, 47(3):455–455, March 1940.

[85] K. Azuma. Weighted sums of certain dependent random variables. *Tohoku Mathematical Journal*, 19(3):357–367, 1967.